AN INVESTIGATION OF PLASTIC BEHAVIOR OF POLYCRYSTALLINE ZIRCONIUM IN THE TEMPERATURE RANGE 4.2°K TO 1032°K

By
V. RAMACHANDRAN

A DISSERTATION PRESENTED TO THE GRADUATE COUNCIL OF
THE UNIVERSITY OF FLORIDA
IN PARTIAL FULFILLMENT OF THE REQUIREMENTS FOR THE
DEGREE OF DOCTOR OF PHILOSOPHY

UNIVERSITY OF FLORIDA
1970

To

My Parents

ACKNOWLEDGEMENTS

The author is very much indebted to Professor R. E. Reed-Hill, Chairman of his Supervisory Committee, for his invaluable guidance, encouragement and stimulating discussions during the course of this research. He is thankful to Dr. C. S. Hartley, Dr. J. J. Hren and Dr. A. K. Varma for serving on his Supervisory Committee. Thanks are due to Mr. A. T. Santhanam for his help during experiments and Dr. D. H. Baldwin and other members of the Mechanical Metallurgy group for their valuable discussions. Dr. T. A. Scott, Professor of Physics, was kind enough to supply liquid helium. Dr. F. N. Rhines, Chairman, Department of Metallurgical and Materials Engineering, was a constant source of inspiration and encouragement throughout the author's stay at the University of Florida.

The financial support provided by the United States Atomic Energy Commission under Contract No. AT-(40-1)-3262 is gratefully acknowledged.

TABLE OF CONTENTS

LIST OF TABLES

LIST OF FIGURES

LIST OF FIGURES - Continued

LIST OF FIGURES - Continued

LIST OF FIGURES - Continued

Abstract of Dissertation Presented to the Graduate Council
in Partial Fulfillment of the Requirements for the Degree of
Doctor of Philosophy
at the University of Florida

AN INVESTIGATION OF PLASTIC BEHAVIOR OF POLYCRYSTALLINE ZIRCONIUM IN THE TEMPERATURE RANGE 4.2°K TO 1032°K

By

V. Ramachandran

March, 1970

Chairman: Dr. R. E. Reed-Hill

Major Department: Metallurgical and Materials Engineering

This study is concerned with the plastic behavior of polycrystalline zirconium over the temperature range 4.2°K to 1032°K. For the tensile tests at 4.2°K, both longitudinal and transverse specimens machined from a rolled zirconium plate were used. In this plate the basal planes of the grains were strongly aligned parallel to and distributed nearly uniformly about the rolling direction. The metal exhibited higher ductility at 4.2°K than at room temperature. Prestraining transverse specimens at 4.2°K produced more room temperature damping capacity than prestraining at 77°K. All stress-strain curves in the 4.2°K tests exhibited characteristic sudden drops in the load, accompanied by audible clicks. Transverse specimens showed a much higher incidence of twinning, greater overall strain hardening, fewer serrations and more plastic deformation between serrations than longitudinal specimens. The present study confirmed Kula and DeSisto's conclusion that twinning per se is probably not the cause for the discontinuous flow. In agreement with

Basinski's hypothesis, the load drops are related to thermal softening during deformation. At temperatures near absolute zero, the heat generated in a specimen during deformation is much more than that necessary to promote an instability and cause a consequent load drop. Hence it is postulated that all the heat generated is not retained in the specimen and a large fraction of it is lost to the surroundings. The experimental evidence suggests that the deformation during a load drop is localized. An estimate of the magnitude of the temperature rise in a typical load drop was made. The effects of recooling the specimen back to 4.2°K after a load drop were analyzed.

Phenomena associated with dynamic strain aging were observed in coarse grained zirconium specimens during tensile tests conducted at elevated temperatures, at two strain rates differing by 3 orders of magnitude. At each strain rate, two peaks characteristic of dynamic strain aging were observed in the flow stress-temperature diagrams. These peaks were found to be strain rate dependent, shifting to higher temperatures with increase in strain rate. A minimum in the strain rate sensitivity of zirconium observed around 675°K is a consequence of the shift in the hardening peak temperature with changes in strain rate. At the temperature of the hardening peak, the tensile elongation of the zirconium specimens showed a minimum at each strain rate. The elongation minima do not reflect a true loss of ductility because the reduction in area did not pass through a corresponding minimum. At the temperature of the hardening peak, there appears to be an increased tendency for neck formation in the tensile specimens. This could be rationalized in terms of variations in the strain rate sensitivity of zirconium caused by dynamic strain aging.

INTRODUCTION

The metal zirconium and some of its alloys find extensive use as structural materials in nuclear reactors by virtue of their good mechanical strength and transparency to thermal neutrons. Large scale development of nuclear power has led to the necessity of a thorough assessment of the properties of these structural materials. Of particular importance is a study of the mechanical behavior of polycrystalline zirconium under various conditions of purity, grain size, texture, temperature and strain rate.

In hexagonal close packed metals such as zirconium, the number of primary slip systems is rather limited. Hence twinning plays a major role in the plastic deformation of such metals especially at low temperatures. Twinning in zirconium and related metals has been the subject of detailed investigation at the University of Florida in the past decade. During this investigation it was found that, at 77°K, operation of this mode has a large influence on the ductility of zirconium. It has also been demonstrated that nucleating $\{11\bar{2}1\}$ twins in suitably oriented specimens by prestraining at 77°K has a beneficial effect on the ability of the metal to damp mechanical vibrations at room temperature. In order to check whether additional improvements in these properties are obtained by deformation at lower temperatures, it was proposed to conduct tensile tests on zirconium at 4.2°K. In this study, certain interesting features peculiar to deformation at extremely low temperatures were observed. Discontinuous plastic flow is the most significant one. These features will be analyzed in terms

of the thermal effects associated with low temperature deformation.

In the course of the investigations at the University of Florida on the plastic deformation of titanium at various temperatures and strain rates, certain anomalies were found at two temperature intervals centered around 250°K and 675°K. These are the temperature ranges in which phenomena associated with dynamic strain aging in titanium also occur. Thus dynamic strain aging can complicate the deformation process in titanium.

Since zirconium is similar in behavior to titanium in many respects, it was proposed to study the flow characteristics of this metal as a function of temperature and strain rate. Phenomena associated with dynamic strain aging were observed also in zirconium, though at different temperature ranges and to different degrees. In addition, another effect observed was that the metal exhibits elongation minima at those temperatures where dynamic strain aging effects are pronounced. Hence it is believed that there may be a close association between dynamic strain aging and the elongation minima in zirconium. These results will be analyzed in terms of the possible mechanisms.

CHAPTER I

PREVIOUS INVESTIGATIONS

1.1. Deformation Mechanisms in Zirconium

Zirconium is known to slip primarily on the $\{10\bar{1}0\}$ prism planes in the $\langle 11\bar{2}0\rangle$ directions.[1,2,3*] Martin and Reed-Hill[4] have shown by tensile tests at 538°C that basal slip may be an important secondary slip mode in zirconium. Baldwin and Reed-Hill[5] were able to identify slip also on the pyramidal planes $\{10\bar{1}1\}$ and $\{11\bar{2}2\}$ in polycrystalline zirconium twisted at 77°K. The twinning modes of zirconium identified by Rapperport[1,2] and also Rapperport and Hartley[3] are $\{10\bar{1}2\}$, $\{11\bar{2}1\}$, $\{11\bar{2}2\}$ and $\{11\bar{2}3\}$. Amongst these the $\{11\bar{2}1\}$ is the most frequently observed mode. The nature of the twinning shear in the three important twin types, namely, $\{11\bar{2}1\}$, $\{10\bar{1}2\}$ and $\{11\bar{2}2\}$ has been described by Reed-Hill.[6]

1.2. Deformation of Metals at Extremely Low Temperatures

During the last two decades there has been a considerable demand for data on low temperature mechanical properties of materials. Certain very interesting features are peculiar to low temperature deformation. In a metal like zirconium, twinning becomes an important mode of deformation at low temperatures. It has been reported earlier that, at 77°K, operation of this mode has a large influence on the ductility of

*Superscript numbers refer to entries in the Bibliography.

zirconium.[7] It has also been shown that nucleating $\{11\bar{2}1\}$ twins in suitably oriented specimens by prestraining at 77°K enhances the damping capacity of the metal at room temperature.[8] Twinning at lower temperatures is generally accompanied by less slip, resulting in less distortion of the matrix. Thus boundaries of twins, nucleated at lower temperatures, may be expected to have higher mobility, enhancing the damping capacity. In order to check whether additional improvements in these properties are obtained by deformation at still lower temperatures, it was proposed to conduct tensile tests on zirconium at 4.2°K.

With the development of the Collins Cryostat which made available bulk liquid helium, a number of metals and alloys have been tested at liquid helium temperature, with a view towards assessing their mechanical properties and also study the deformation mechanism. "Research on the mechanical properties of metals at liquid helium temperatures" has been the subject of a detailed review by Rosenberg.[9] Deformation in metals, including zirconium, at temperatures near absolute zero is characterized by discontinuous plastic flow. This is manifested in the appearance of serrations or sudden load drops in a tensile load-elongation curve, after the initial yielding. Serrations in the stress-strain curves have been observed in aluminum and 24S aluminum alloy by Basinski;[10] in copper by Blewitt, Coltman and Redman;[11] in nickel, zirconium, beta brass and SAE 3335 and 4340 steels by Wessel;[12] in K-Monel, Armco iron, tantalum-10 percent tungsten alloy, titanium and AISI 416 steel by Kula and DeSisto;[13] in lithium by Hull and Rosenberg;[14]

in cupronickel by Erdman and Jaheda;[15] and in certain stainless steels by Collins et al.[16]

A number of theories based on deformation twinning,[17] dislocation bursts[12] and phase transformations[14,18] have been proposed to explain the discontinuous plastic flow. Basinski's theory[10] based on localized heating of the test specimen during deformation is perhaps the most generally accepted one. Basinski found discontinuous flow in super pure aluminum at 4.2°K. Since aluminum is unlikely to form a martensite and because of its high stacking fault energy is also unlikely to twin, Basinski recognized that the serrated flow curve of aluminum is most likely to be associated with discontinuous slip. At extremely low temperatures, metals have a very low heat capacity. Part of the energy of deformation, which is not stored in the specimen, is converted into heat. Due to the very low heat capacity, the heat generated causes an appreciable temperature rise in the specimen. The flow stress of metals, in general, decreases rapidly with increase in temperature in this region. The rise in temperature of the specimen can cause its flow stress to fall below the applied stress, thus causing an instability. This is a thermal softening effect. Basinski was the first to measure the time taken for a load drop and also estimate the temperature rise during a load drop. According to him the deformation will become unstable provided that the localized heating can produce an appreciable softening of the metal and that the heat produced during the deformation can be localized at least for the time necessary for the flow to occur. With materials of very low thermal conductivities at

4.2°K, such as aluminum-2 percent magnesium alloy and solution treated 24S alloy, discontinuous yielding was found to be more pronounced. The localization of the instantaneous heat sources during the discontinuous flow of a copper-nickel alloy at 4.2°K has been recognized by Erdman and Jahoda[15] by transient calorimetry.

Wessel[12] explored the tensile properties of nickel, zirconium, beta brass and SAE 3335 and 4340 steels, thus covering three different crystal structures, at temperatures down to that of liquid helium. Discontinuous flow was exhibited by all these materials at 4.2°K. He considers the possibility of thermal instability at these low temperatures being the cause of the discontinuities, as suggested by Zener and Hollomon.[19] The high flow stress of metals at low temperatures combined with low specific heats and low thermal conductivities obtaining at these low temperatures could cause considerable local heating. However, he questions this localized heating as a possible mechanism for nickel and zirconium whose flow stresses are relatively less temperature sensitive than the b.c.c. metals. To explain the serrated stress-strain curves for many metals of different crystal structures, a general mechanism is necessary. Wessel considers that repeated yielding at very low temperatures may be the result of bursts of dislocations. The high stresses required for the release of a dislocation at very low temperatures may be sufficient to trigger a burst of dislocations causing considerable plastic deformation. When these dislocations interlock, plastic flow would stop. On reloading, a new source might be activated elsewhere to produce a new burst.

According to Powell, Marshall and Backofen,[18] the serrations at 10°K in the stress-strain curves of 301 and 304 type stainless steels may well be due to martensitic transformation though a more important reason would be localized thermal softening. Amongst the alkali metals studied by Hull and Rosenberg,[14] lithium exhibited discontinuous flow at 4.2°K. Lithium transforms from b.c.c. to h.c.p. structure below 72°K without cold work. The discontinuous flow in lithium has been attributed to a catastrophic transformation from h.c.p. to a f.c.c. structure.

Under certain conditions discontinuous flow may be due to twinning as for example in single crystals. However, in polycrystalline titanium, that is similar in its mechanical behavior to zirconium, Kula and DeSisto[13] have concluded that twinning per se may not be responsible for the load drops. This was because they observed twinning at 4.2°K both before and after the first serration. Their view is further strengthened by the results on the deformation of copper single crystals at 4.2°K by Blewitt, Coltman and Redman.[11] According to them, the deformation is believed to proceed by three different mechanisms, namely, ordinary glide at low flow stresses, discontinuous slip or serrated flow at intermediate flow stresses and twinning at high flow stresses for crystals of appropriate orientations. Once the crystal is completely twinned, it continues to deform again by discontinuous slip. The discontinuous slip occurs as a result of an avalanche of slip lines, with approximately 30 slip lines released for each discontinuity in the flow curve, with each line producing a displacement of 2×10^4 Å. No twinning could be detected in the

discontinuous slip region. In order to check Kula and DeSisto's hypothesis with regard to the role of twinning in discontinuous yielding, it was decided to compare the deformation behavior of polycrystalline zirconium of two basically different orientations. In one of these orientations deformation at small strains depends primarily on twinning, and in the other, on slip.

The load drop was found to occur very rapidly, in about 1.5×10^{-4} sec.[10] During this small time interval, the total distance between the crossheads of the testing machine remains practically constant, or increases by a distance consistent with the crosshead speed. A drop in load must be accompanied by an elastic relaxation of the specimen and the system. Hence there must be a plastic extension of equal magnitude in the specimen to keep the total length constant or increasing at the crosshead speed. There is thus an exchange of plastic strain for elastic relaxation accompanying each load drop. Deformation during load drops is believed to be localized in a fraction of the gage length. Collins et al.[16] have reported a sudden localized elongation of about 0.005 in. for each discontinuity in the load-elongation curve of stainless steels. Kula and DeSisto[13] report necking associated with each serration in the case of AISI 416 steel. Therefore it was felt that a study of the strain distribution along the length of a specimen might be able to provide additional information about the localization of the flow during load drops.

Though it is generally believed that load drops are caused by heating of the test specimen during deformation, there are still certain

aspects of this assumption that have not been completely explained. For example, the effect of heating and the consequent thermal softening is likely to be greatly influenced by the heat loss from the specimen. This has been neglected by earlier workers. In the case of titanium, Kula and DeSisto's[13] estimation of thermal softening predicts a load drop even in the microstrain region, whereas they observed the first load drop after a small but finite strain. There are many other materials such as aluminum,[10] copper,[11] nickel,[12] K-Monel,[13] lithium,[14] cupronickel,[15] stainless steels[16] and 2024 aluminum alloy[20] in which the serrations start only after considerable plastic deformation. These examples imply that Kula and DeSisto's relation does not accurately predict the occurrence of the first load drop. It was proposed to check whether this is also true in the case of zirconium and if so to explore the possible cause for this inconsistency.

1.3. Deformation of Metals at Higher Temperatures

In the study of the plastic behavior of a metal over the temperature range from near absolute zero to its melting or transformation temperature, one generally passes through a temperature range where the deformation is complicated by dynamic strain aging. This process is very common in metals and it is difficult to find materials in which some of its aspects do not appear. Zirconium is not an exception. In plastic deformation studies, the most important experimentally measured parameter is the flow stress. Hence an understanding of the flow stress of a metal and its variation with temperature is of great importance in understanding dynamic strain aging. In this section the general

theory of flow stress and its relation to dynamic strain aging will be described with a review of the earlier work in this area.

1.3.1. Components of Flow Stress

In a nearly pure metal, the flow stress σ in a tensile test is composed of two basic components.[21] One is that necessary to move dislocations against the action of the long range strain fields of the other dislocations. This component, denoted by σ_ℓ, is often referred to in literature as the "athermal component" as it is believed not to be directly controlled by thermal activation. Its dependence on temperature is only through the shear modulus. The remaining part of the flow stress is the short range component, σ_s, which acts over a few atomic diameters only. This may be interpreted as a friction stress due to the resistance offered by the lattice to dislocation motion. Thermal activation is necessary to overcome such obstacles and hence σ_s is referred to as the thermally activated component. This component becomes prominent at low temperatures. One can therefore write for a nearly pure metal,

$$\sigma = \sigma_s + \sigma_\ell \quad . \tag{1}$$

Dingley and McLean[22] have shown, in 99.97 percent pure iron, that the long range component σ_ℓ of the flow stress is related to the total dislocation density ρ according to the equation,

$$\sigma_\ell = K\rho^{1/2} \tag{2}$$

where K is a constant. According to Johnston,[23] in lithium fluoride,

the dislocation velocity v depends on the applied shear stress τ according to a power law

$$v = \left(\frac{\tau}{D}\right)^m \tag{3}$$

where D is a constant. In this case, the short range component is related to the mobile dislocation density by the equation

$$\sigma_s = D\left(\frac{\dot{\varepsilon}}{\rho_m b}\right)^{\frac{1}{m}} \tag{4}$$

where $\dot{\varepsilon}$ is the strain rate, ρ_m the mobile dislocation density, b the Burgers vector and m the dislocation velocity exponent. Reed-Hill[24] has shown that this may be true in the case of titanium in the strain interval from 1 percent to 12 percent.

The flow stress of metals measured at a constant strain rate generally decreases with temperature and then tends to be temperature independent at moderately high temperatures. In this region, based on the assumption that the long range component is athermal, Seeger[21] has concluded that the thermally activated component vanishes and hence the total flow stress σ equals the long range component σ_ℓ. Extending this assumption below this "athermal" region, the thermally activated component has been obtained by subtracting this constant value of σ_ℓ from the total flow stress, of course after making a correction for the temperature dependence of the modulus.[25,26] Reed-Hill[24] has shown that this assumption is probably not justified since the phenomena associated with this temperature range are too complex to be ignored or to be explained in such a simple manner. He has also pointed out that the

practice of obtaining the thermally activated component by subtracting a constant "athermal" stress component from the total flow stress is open to serious question.

If the long range component is due to the interactions of the dislocations, and hence governed by the total dislocation density, then under conditions of low dislocation density, the total applied flow stress might very closely approximate the thermally activated component. In practice, such conditions may be obtained in two ways. One is by measuring the flow stress at very small strains, say 0.2 percent at which there may not be a heavy build-up of dislocation density.

There is experimental evidence that fine grained specimens develop much higher dislocation densities than coarse grained ones.[22,27] The Petch effect is directly related to this. Hence the higher flow stress of fine grained specimens is due to an increase in σ_i with decreasing grain size. Therefore in coarse grained specimens the flow stress at small strains is more characteristic of the thermally activated component.

In a metal that exhibits a sharp yield point, a very rapid change in dislocation density by over several orders of magnitude is implied.[23] This can produce a strong discontinuity in the short range component. In titanium and zirconium, yield points are usually observed only in specimens of very small grain sizes, whereas coarse grained specimens normally tend to undergo continuous yielding.[25,28] According to Weinstein,[28] coarse grained zirconium specimens may have a relatively large initial mobile dislocation density which according to Hahn's[29]

analysis should result in a smaller yield drop or complete disappearance of the yield point.

1.3.2. Temperature Dependence of Flow Stress

The flow stress in many metals tends to decrease exponentially with the absolute temperature[30-35] so that the flow stress data at small strains for coarse grained specimens may be expressed empirically as

$$\ln \frac{\sigma_s}{\sigma_{s_o}} = -BT \tag{5}$$

where σ_s is the flow stress, σ_{s_o} the flow stress at absolute zero, B a constant and T the absolute temperature. The data of Carreker[30] on platinum and of Baldwin and Reed-Hill[31] on a series of zirconium-oxygen alloys obtained under these experimental conditions provide examples of this behavior.

1.3.3. Activation Energy

Suppose the plastic strain rate $\dot{\epsilon}$ conforms to an Arrhenius equation

$$\dot{\epsilon} = Ae^{-H/RT} \tag{6}$$

where A is a parameter depending on several factors including the mobile dislocation density and H the activation enthalpy and R the universal gas constant. This gives for H,

$$H = -RT\ln\left(\frac{\dot{\epsilon}}{A}\right) . \tag{7}$$

At constant strain rate, if A is assumed constant, the activation enthalpy H must vary directly with the absolute temperature T. By equation 5, $\ln \frac{\sigma_s}{\sigma_{s_o}}$ also varies directly as T. Hence one can write

$$H = H_o \ln \frac{\sigma_{s_o}}{\sigma_s} \tag{8}$$

where H_o is a constant.

1.3.4. Strain Rate Sensitivity

Substituting the expression for the activation enthalpy in the plastic strain rate equation 6 gives

$$\dot{\varepsilon} = Ae^{-\frac{H_o}{RT} \ln \frac{\sigma_{s_o}}{\sigma_s}} = A\left(\frac{\sigma_s}{\sigma_{s_o}}\right)^{\frac{H_o}{RT}} . \tag{9}$$

Or,

$$\sigma_s = \sigma_{s_o}\left(\frac{\dot{\varepsilon}}{A}\right)^{\frac{RT}{H_o}} . \tag{10}$$

This is of the same form as the power law equation 4 obtained by Johnston and Gilman,[36] relating the strain rate to the applied stress through the dislocation velocity exponent, m. Hence

$$m = \frac{H_o}{RT} . \tag{11}$$

If A is independent of strain rate and temperature, then for two strain rates, $\dot{\varepsilon}_1$ and $\dot{\varepsilon}_2$,

$$\frac{\dot{\varepsilon}_2}{\dot{\varepsilon}_1} = \left(\frac{\sigma_{s_2}}{\sigma_{s_1}}\right)^{\frac{H_o}{RT}} \tag{12}$$

or

$$\frac{\sigma_{s_2}}{\sigma_{s_1}} = \left(\frac{\dot{\epsilon}_2}{\dot{\epsilon}_1}\right)^{\frac{RT}{H_o}} \quad . \tag{13}$$

This implies that $\frac{RT}{H_o}$ equals the strain rate sensitivity parameter, n, under conditions of negligible long range flow stress component. Hence the strain rate sensitivity parameter should vary directly as T. Carreker's[30] data on coarse grained platinum conform closely to this relation.

Monteiro, Santhanam and Reed-Hill[37] have found that in commercial purity titanium, the strain rate sensitivity data deviated from this theoretical straight line to lower values in two temperature ranges centered around 250°K and 670°K. These are the temperature ranges in which several abnormalities are observed in the plastic deformation behavior of titanium. These abnormalities have been attributed to the phenomenon of dynamic strain aging which makes the plastic behavior quite complex. The various attributes of dynamic strain aging are discussed in the next section.

1.3.5. Dynamic Strain Aging

Strain aging is a well-known phenomenon that occurs in many materials, including mild steel. When a specimen is deformed beyond the yield point, unloaded and then reloaded, a sharp yield point is not observed. However, if the specimen is aged sufficiently in the unloaded condition and tested again, the yield point returns. At those temperatures where it is normally studied, this phenomenon

usually occurs over a finite period of time so much so it is basically a static process. For example, in the case of mild steel, it may take a few days at room temperature for the yield point return. Strain aging can be explained in terms of dislocation pinning by diffusing impurity atoms,[38] so that the kinetics of the process should depend largely on the diffusion rates of the impurity atoms. As a result, strain aging phenomena may occur simultaneously with deformation if the temperature is suitably raised. When this happens the metal is said to undergo dynamic strain aging. The dynamic aspects of strain aging[39,40] that have been identified are (a) the appearance of plateaus or peaks in flow stress-temperature diagrams, (b) discontinuous yielding or the Portevin-Le Chatelier[41] phenomenon, (c) abnormally low strain rate sensitivity, (d) abnormal work hardening rates and (e) ductility minima. Dynamic strain aging manifests itself, at least to some degree, in one or more of these aspects in most metallic materials.

A striking example from recent work in this area is the study of the variation of the compressive flow stress of columbium with temperature at various strain rates, by Wessel, France and Begley,[40] which is shown in Fig. 1. They observed that the flow stress, instead of decreasing steadily with a rise in temperature, showed peaks at intermediate temperatures. Two peaks were obtained at a strain rate of 10^{-4} sec^{-1}; one at about 230°C and the other at 400°C. On increasing the strain rate by a factor of 10, the peaks moved to higher temperatures, namely, about 300°C and 450°C respectively. The same trend was noticed on further increase of strain rate. These peaks, which will be referred

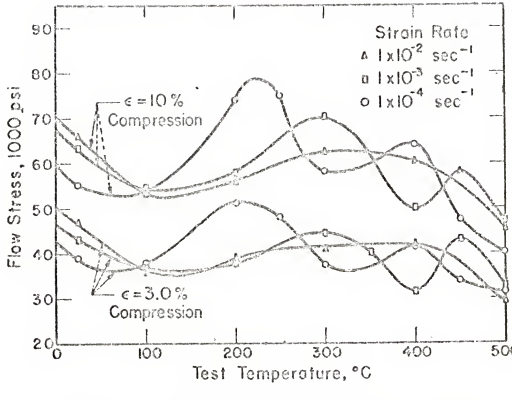

Figure 1. Effect of strain rate on the flow stress of Cb in the temperature range 0 to 500°C.*

(* E. T. Wessel, L. L. France and R. T. Begley, Columbium Metallurgy, p. 495, Interscience Publishers, New York, 1961)

to as hardening peaks, are therefore strain rate dependent. Wessel, France and Begley attributed the lower temperature peak to oxygen atoms in solution, and the higher temperature peak to nitrogen and/or carbon in solution.

Similar shifts in hardening peak temperatures with changes in strain rate have also been reported in mild steel by Manjoine[42] and Nadai and Manjoine,[43] and in Fe-N as well as Fe-Mn-N alloys by Baird and Jamieson.[44] In the h.c.p. metal titanium, two hardening peaks have also been observed by Monteiro, Santhanam and Reed-Hill.[45] They used specimens of 16 μ grain size which were tested in tension between 77°K and 1133°K at strain rates varying through 5 orders of magnitude.

Usually at or around the temperature of the hardening peak, the other aspects of dynamic strain aging are also observed. Thus Owen and Roberts[46] found a plateau in the flow stress-temperature plot of a nickel steel. In the same temperature range of approximately 70°C to 170°C, serrated flow was observed at a strain rate of 8.3×10^{-5} sec^{-1}. On a tenfold increase of strain rate, the region of serrated flow shifted to the interval 100°C to 200°C.

Dynamic strain aging effects appear to be the rule rather than the exception in metals. Their significance, especially that of the hardening peaks, has been more or less ignored. Since work on this feature of the plastic behavior of zirconium has been rather meagre, it was proposed to study this aspect by conducting tensile tests on coarse grained zirconium specimens over a wide range of temperature and

strain rate. The details of these investigations are described in the following chapters.

CHAPTER II

EXPERIMENTAL METHODS

2.1. Deformation at 4.2°K

2.1.1. Material

To study the possible role of twinning in causing discontinuous flow at extremely low temperatures, it was proposed to compare the deformation behavior of polycrystalline zirconium specimens of two basically different orientations, as mentioned in the previous chapter. Such specimens were obtained from zirconium plate of a specific texture. The zirconium used in the low temperature work was arc-melted sponge zirconium with an ASTM grain size 6 obtained from Wah Chang Corporation in the form of a 1/2 in. thick plate. The analysis of this metal is given in Table 1. The plate had a texture with the basal planes of the grains strongly aligned parallel to the rolling direction. The basal poles were uniformly distributed about the rolling direction. This is similar to a wire texture, common in commercially available zirconium plate. This texture is shown schematically in Fig. 2. Longitudinal and transverse specimens were machined from this plate. In the longitudinal specimens, most grains have their basal planes parallel to the stress axis. This favors prism slip and $\{11\bar{2}2\}$ twinning. On the other hand, in transverse specimens, the angle between stress axis and basal pole varies over a wide range and a finite fraction of the grains are unfavorably oriented for prism slip. As a result, twinning on $\{10\bar{1}2\}$ and $\{11\bar{2}1\}$ should play an important role in the deformation of

TABLE 1

COMPOSITION OF ARC-MELTED SPONGE ZIRCONIUM

Element	Composition (parts per million)	Element	Composition (parts per million)
Al	44	Mo	< 10
B	< 0.2	N	39
C	110	Ni	10
Cd	< 0.3	O	965
Co	< 5	Pb	< 5
Cr	< 10	Si	71
Cu	25	Sn	< 10
Fe	435	Ti	< 20
Hf	< 40	V	< 5
Mg	< 10	W	30
Mn	< 10	Zn	< 50

Balance zirconium

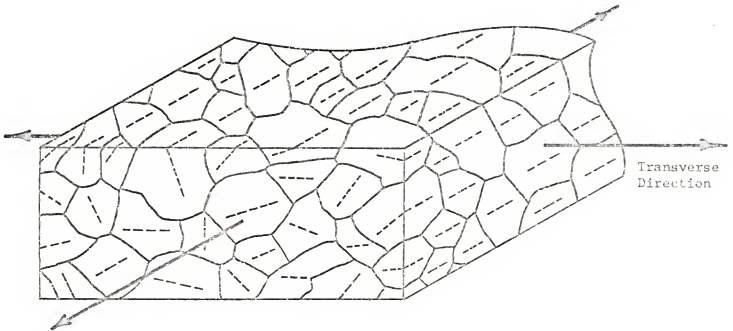

Figure 2. Schematic representation of the zirconium plate texture.* The basal plane trace is indicated by a dashed line in each grain. Note that the basal planes tend to be parallel to the rolling direction while distributed uniformly about it.

(* J. L. Martin and R. E. Reed-Hill, Trans. Met. Soc. AIME, 1964, vol. 230, p. 781)

transverse specimens.[6] Thus a basically different deformation behavior is expected for the two specimen types. The relationship of this difference to the plastic deformation of zirconium at 4.2°K is part of the present investigation.

2.1.2 Specimen Preparation

Standard 1/8 in. gage diameter tensile specimens of the form described by Rittenhouse and Picklesimer[47] were prepared from the plate stock. Pieces 1/2 x 1/2 x 3-1/2 in. were sawed off from the plate. On one end of each piece, marks were scribed as shown in Fig. 3 so that the rolling direction and the rolling plane normal could be identified on the finished specimen. The pieces were turned into blanks 3 in. long with 1/2 in. of 1/4 - 20 threads at either end and a reduced section of 3/16 in. diameter.

The final gage section of approximately 0.128 in. diameter was formed by chemical machining. The machining solution consisted of 5 parts by volume H_2O, 4 parts HNO_3, 2 parts HCl and 1 part HF. The ends of the specimen were coated with paraffin wax. The specimens were then gently rolled in the acid bath. When freshly prepared, the acid removed the metal at the rate of 0.001 in. per minute. Machining was stopped after every 5 minutes, the specimens were washed in running cold water, dried and the diameter of the gage section measured with a micrometer. Undercutting by the acid was prevented by fresh waxing of the ends. After the final acid machining which removed about 0.008 in. of the metal, the diameters in two perpendicular directions were measured at

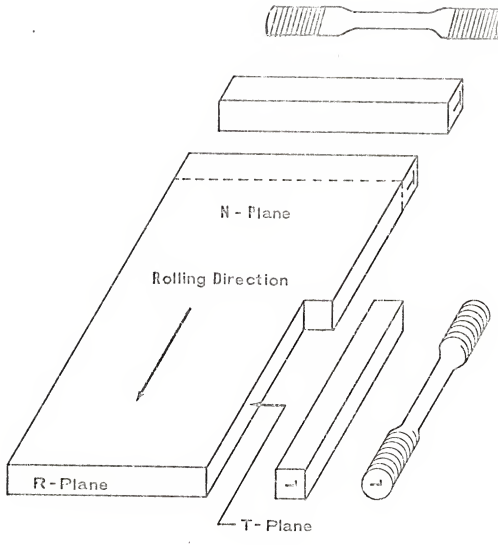

Figure 3. Orientation of the tensile test specimens with respect to the original plate.

intervals along the gage section. For this, a Jones and Lamson optical comparator of accuracy 0.0001 in. was used instead of the micrometer to preclude surface damage by the micrometer anvils. The diameter was found to be fairly uniform along the gage length, with a variation of less than 0.002 in. The final gage length was nominally 1-1/4 in. measured at the bottom of the fillets. The geometry of the specimen is indicated in Fig. 4. The microstructure of the acid machined specimen was initially deformation free as seen in Fig. 5.

2.1.3. Apparatus

The tensile tests were conducted in a TTC model Instron machine of 10,000 lbs capacity. The cryogenic accessories are shown in Fig. 6. The specimen was connected to the load cell of the machine through a stainless steel pull rod, and the other end was attached, through a collar and hemispherical seating which served as the bottom grip, to the rigid bottom of a stainless steel pulling tube. The bottom grip assembly was tied to the stainless steel tube with a wire so that it would not fall inside the Dewar when the specimen broke. The pulling tube was screwed on to the bottom surface of the crosshead as shown in Figs. 7 and 8. The tube was introduced into a double Dewar cryostat as shown in Fig. 9 and the system was cooled with liquid nitrogen for several hours. Minutes before the test, the liquid nitrogen from the inner Dewar was pumped out and liquid helium was then transferred in from a tank. The outer Dewar was always kept filled with liquid nitrogen. The stainless steel tube had several holes in it so that liquid helium

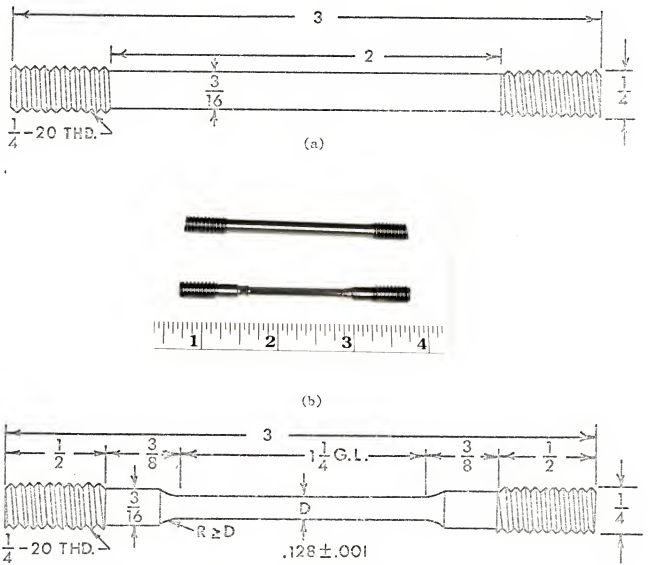

Figure 4. Dimensions of the tensile specimen before and after chemical machining.

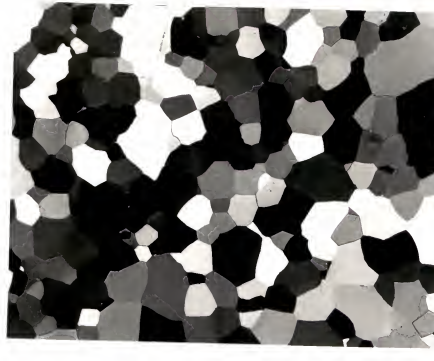

Figure 5. Microstructure of the chemically machined zirconium tensile specimen surface. Polarized light. Magnification 300 times.

Figure 6. Cryogenic accessories: Pulling tube, grips and pull rod.

Figure 7. Pulling tube attached to the crosshead of the testing machine.

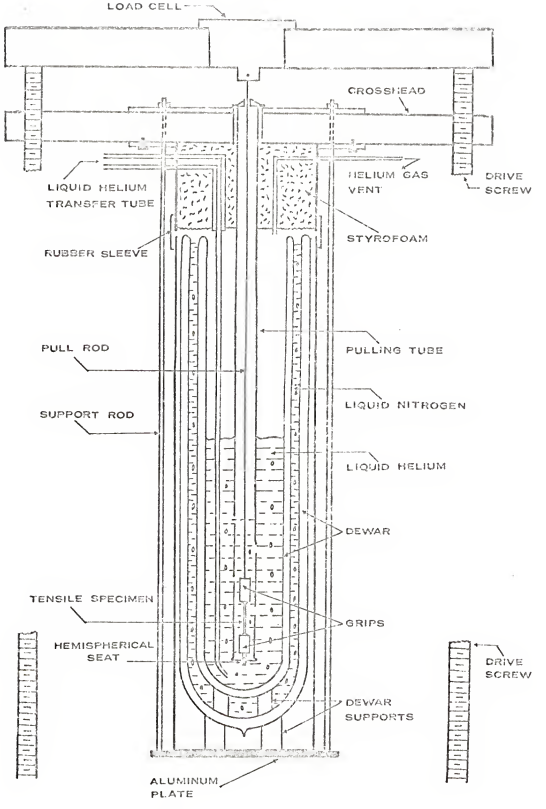

Figure 8. Schematic drawing of the 4.2°K tensile testing apparatus.

Figure 9. Double Dewar cryostat ready for tensile testing at 4.2°K.

could enter the tube and continuously surround the specimen. After the vigorous boiling of liquid helium had subsided and the liquid level had become almost steady, the tensile test was started. Both longitudinal and transverse specimens were tested at a constant crosshead speed of 0.02 in. min^{-1}, corresponding to an initial strain rate of 2.6×10^{-4} sec^{-1}.

After the test, the specimens were carefully removed. As a result of the deformation, their cross sections became slightly elliptical. This was due to a small strain anisotropy in the cross section. The diameters were measured along the major and minor axes of the ellipse, at intervals along the gage section using the optical comparator. The specimens were then sectioned, mounted in epoxy cold mount in such a way that the surface of metallographic examination would be a plane perpendicular to the rolling plane. This was done because on such planes the extinction under polarized light is sharp. The specimen was metallographically polished and etched in a solution containing 5 parts HNO_3, 5 parts H_2O and 1 part HF, and immediately anodized. Anodizing increases the sensitivity of the zirconium surface to polarized light, thereby permitting the basal plane trace orientation in a grain or twin to be easily determined. The anodizing bath had the following composition:[48] ethyl alcohol 120 ml, distilled water 70 ml, glycerine 40 ml, lactic acid 20 ml, orthophosphoric acid 10 ml and citric acid 4 g. The cathode was stainless steel and the potential was 24 volts. Anodizing was stopped when the surface attained a pinkish blue tinge. This usually takes about 4 seconds. The orientation of twins was determined

by the single surface technique of Reed-Hill and Baldwin[49] using the polarized light microscope and the volume fraction of twins by the standard point count method.[50]

2.2. Deformation at Higher Temperatures

2.2.1. Material

As mentioned in section 1.3.1., it was felt desirable to use coarse grained specimens for studying the plastic behavior of zirconium over the wide temperature range envisaged. It was proposed to produce coarse grains by the strain anneal technique similar to that used by Bokros.[51] For this, zirconium stock of fine grain size was necessary. Reactor grade zirconium was obtained from Reactive Metals, Inc., in the form of 5/8 in. diameter bars. The average ingot composition of the metal is given in Table 2. The bars were swaged in a Fenn Rotary Swaging Machine to 75 percent reduction in area. Tensile specimens of the geometry indicated in Fig. 4a were machined from the swaged rods. These were recrystallized by annealing for one hour at 580°C in evacuated Pyrex capsules, gettered with tantalum and zirconium. This resulted in a grain size of about 10 μ. These specimens were then strained in an Instron machine to a critical strain of 5.5 percent and re-annealed in vacuum for 200 hours at 570°C using gettered quartz capsules. This treatment produced a uniform grain size of about 150 μ as measured by the lineal intercept method.

2.2.2. Specimen Preparation

The 1-1/4 in. long by 1/8 in. diameter gage sections were

TABLE 2

AVERAGE INGOT ANALYSIS OF REACTOR GRADE ZIRCONIUM

Element	Composition (parts per million)	Element	Composition (parts per million)
Al	28	Mo	< 20
B	.27	N	36
C	149	Na	< 10
Ca	< 20	Ni	< 20
Cd	< .25	O	1050
Co	< 10	Pb	< 20
Cr	< 20	Si	49
Cu	< 20	Sn	< 20
Fe	260	Ti	< 20
H	10	U	< .2
Hf	84	V	< 20
Mg	< 10	W	< 20
Mn	< 20		

chemically machined as described in section 2.1.2. Since chemical machining tends to introduce surface hydrides in this grade of material, the gage sections were finished by electropolishing at -55°C in a bath of 59 parts by volume methanol, 35 parts n-butanol and 6 parts $HClO_4$ using a zirconium cathode. Cooling of the electrolyte was necessary because of its explosive nature.

2.2.3. Apparatus

After measuring the diameter at intervals along the finished gage section, the specimens were tested in an Instron machine at two different strain rates, 1.3×10^{-5} sec^{-1} and 1.3×10^{-2} sec^{-1}, at temperatures from 77°K to 1032°K. At 77°K and 193°K, the test specimen was immersed in liquid nitrogen and dry ice in acetone respectively, in a Dewar flask. For the tests above room temperature, the high temperature vacuum capsule of the Instron, shown with accessories in Fig. 10, was modified to admit inert atmosphere continuously throughout the test. The specimen was attached to threaded grips inside this capsule surrounded by an electric furnace, mounted on the crosshead as shown in Fig. 11. The capsule was filled with pure dry argon atmosphere desiccated through concentrated H_2SO_4 and anhydrous $CaSO_4$, and deoxygenated by passing through hot zirconium chips. Temperature was controlled by two variacs set for high and low voltages and a switching mechanism. The specimen was surrounded by a tantalum tube filled loosely with clean dry zirconium chips. The temperature of the specimen was measured by a thermocouple placed near the center of the gage

Figure 10. High temperature tensile testing capsule, pull rod and grips.

Figure 11. Assembly for high temperature tensile testing.

section. The temperature variation during a test was less than 1°C. The two ends of the capsule were kept cooled by water jackets. The capsule was fitted with a sliding O-ring seal. The gripping mechanism inside the capsule was provided with enough mechanical slack, so that, in each test, the friction force of the sliding O-ring could be measured and recorded before the specimen was loaded. This friction load was later subtracted from the total load to give the actual load on the specimen.

CHAPTER III

EXPERIMENTAL RESULTS

The data obtained from the present experiments are presented graphically in this chapter. Some numerical values are given in the Appendix.

3.1. Deformation at 4.2°K

3.1.1. Mechanical Properties

In Table 3, the mechanical properties of zirconium at 4.2°K are summarized. The important feature to be noted is the high ductility exhibited by both specimen types. Below room temperature, many metals tend to lose their ductility and become brittle, whereas zirconium has enhanced ductility at low temperatures. Elongation values at 4.2°K are about 25 percent larger than at 300°K. It is believed that the high ductility is associated with the ability of the metal to twin at low temperatures. Twinning adds additional operating deformation modes over and beyond those associated with slip, and these might be expected to enhance ductility.

TABLE 3

MECHANICAL PROPERTIES OF ZIRCONIUM AT 4.2°K

Type of Specimen	0.2% Yield Strength (psi)	Ultimate Strength (psi)	Elongation (%)
Longitudinal	64,000	114,700	26
Transverse	87,000	126,900	25

3.1.2. The Effect of Prestraining at 4.2°K on the Room Temperature Damping Properties

It has been demonstrated earlier by Reed-Hill, Dahlberg and Slippy[8] that nucleation of thin $\{11\bar{2}1\}$ twins in transverse zirconium specimens by small prestrains at 77°K can markedly increase the room temperature damping capacity of this metal. In order to see if this effect is also observed by prestraining at 4.2°K, a transverse specimen was deformed about 0.86 percent in liquid helium. This induced many thin $\{11\bar{2}1\}$ twins, their volume fraction being 0.06. Strain gages of 'MA' Series, supplied by Micro-Measurements, Inc., were attached to this specimen and the room temperature mechanical hysteresis was studied by deforming the specimen to about 15,000 psi, unloading and reloading to the same stress level. The cyclic energy loss was found to be about 50 percent greater than for a specimen prestrained 0.64 percent at 77°K, at which strain the hysteresis loss was a maximum for this prestraining temperature. The volume fraction of $\{11\bar{2}1\}$ twins in the latter specimen was 0.08. This comparison is illustrated in Fig. 12.

3.1.3. Discontinuous Flow

The load-elongation curves of both longitudinal and transverse specimens had characteristic saw-toothed serrations. Loud clicks were heard whenever a load drop occurred. A typical transverse specimen curve is shown in Fig. 13 plotted on true stress-true strain coordinates. After an initial smooth continuous plastic deformation of about 4 percent, serrations appear and deformation proceeds by a series of

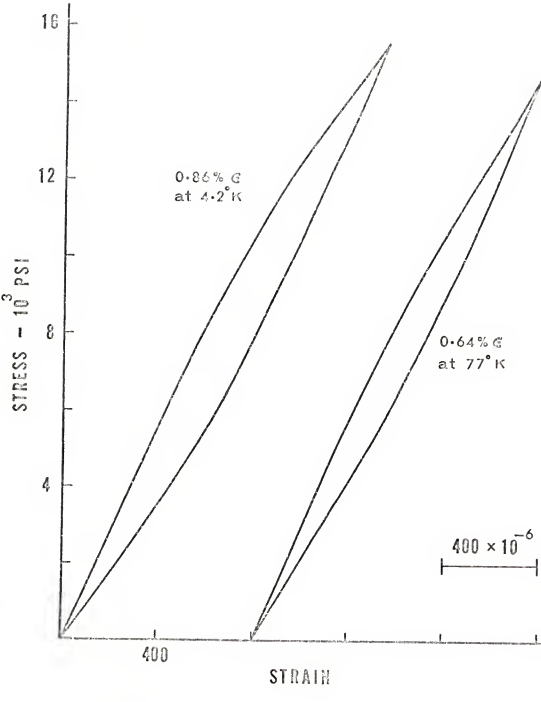

Figure 12. Hysteresis loops of zirconium specimens prestrained at 4.2° and 77°K.

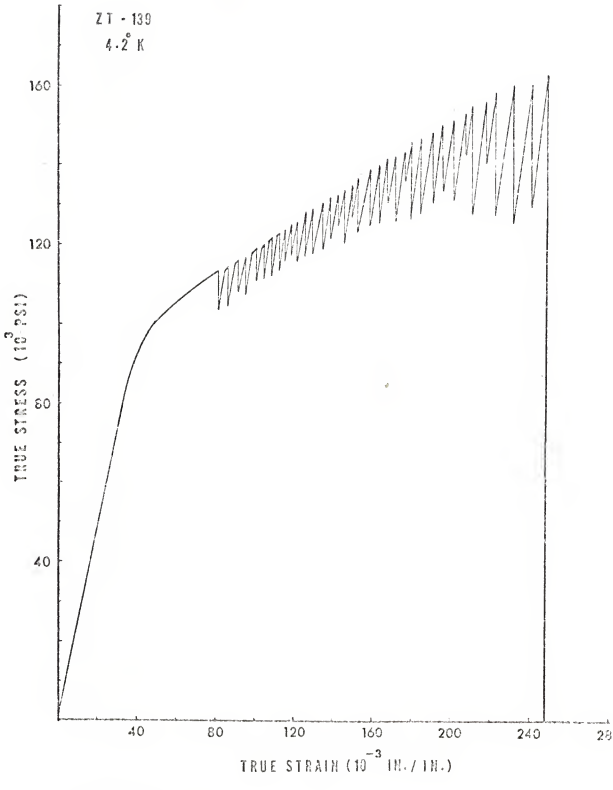

Figure 13. True stress-true strain curve of the transverse zirconium specimen deformed at 4.2°K.

discontinuous yielding events. It may be noted, from the general overall slope of the stress-strain curve, that there is appreciable work hardening in the transverse specimen. After each load drop, there is elastic deformation followed by a variable finite amount of plastic deformation prior to the next load drop. Load drop occurred 35 times before the specimen fractured.

Figure 14 is a tracing of portions of the Instron charts of the two kinds of specimens. As may be seen in the upper curve between points B and C, D and E, and F and G, the work hardening rate in the transverse specimen is apparently higher between load drops than during continuous flow prior to the first load drop. Also, this work hardening rate is not the same in all intervals between serrations.

Figure 15 shows the stress-strain curve of a longitudinal specimen. Here, serrations start at about 1.4 percent plastic strain and the general work hardening rate is lower than in the transverse specimen. The frequency of load drops is however greater, being 59 before fracture. Also after each load drop, the deformation is largely elastic with much less plastic deformation than in the transverse specimen. Most of these details may be seen in Fig. 14.

3.1.4. Metallographic Studies

In order to check whether observable microstructural changes such as deformation twinning were associated with load drops, two longitudinal specimens were tested. One was deformed to a strain estimated to be almost equal to that needed to cause a serration and

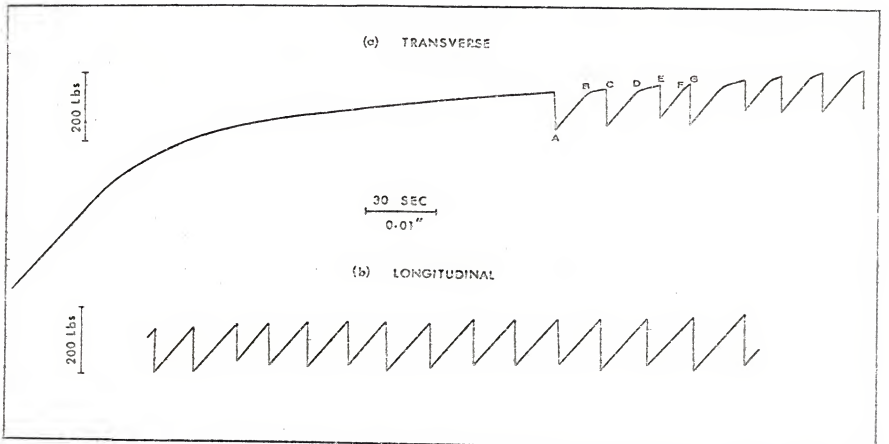

Figure 14. Portions of the Instron load-time charts of the transverse and the longitudinal specimens.

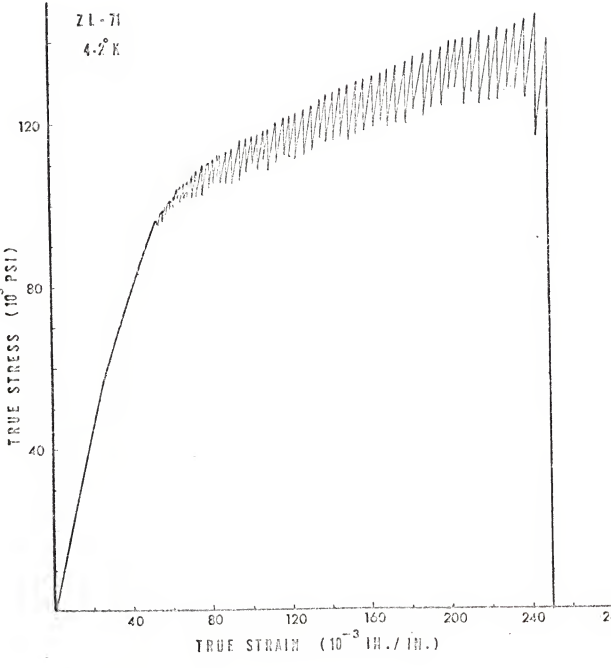

Figure 15. True stress-true strain curve of the longitudinal zirconium specimen deformed at 4.2°K.

another was deformed to a strain sufficient to produce only a single serration. The corresponding plastic strains were 0.6 percent and 1.4 percent. Twinning was observed even in the specimen without the serration. A gage section survey was made by the method shown schematically in Fig. 16. From a total of N grains intercepted by a line of constant length, the number of grains containing twins (n) was counted and the fraction of grains containing twins was taken as n/N. This quantity was measured along the entire gage section. It was found that 3 percent of the grains contained twins and that these latter were more or less uniformly distributed over the gage length. Figure 17 shows a typical micrograph of this specimen. Note the twins in one grain. Most twins were $\{11\bar{2}1\}$ and occurred in grains with basal planes nearly perpendicular to the stress axis and thus in the small number of grains not conforming to the basic texture. This was determined by polarized light microscopy. However, a few grains with $\{11\bar{2}2\}$ and $\{10\bar{1}2\}$ twins were observed. The total volume fraction of twins was very small.

Figure 18 shows the microstructure of the longitudinal specimen deformed only enough to produce a single serration. Near the bottom of the figure is a grain whose basal plane was nearly perpendicular to the stress axis. It contains a number of $\{11\bar{2}1\}$ twins. Note that they are characteristically thin and zig-zag in appearance. This grain also deviates from the basic texture. The grain at the center exhibits $\{11\bar{2}2\}$ twins and has its basal plane nearly parallel to the stress axis. In this case the grain conforms to the texture. Figure 19 shows

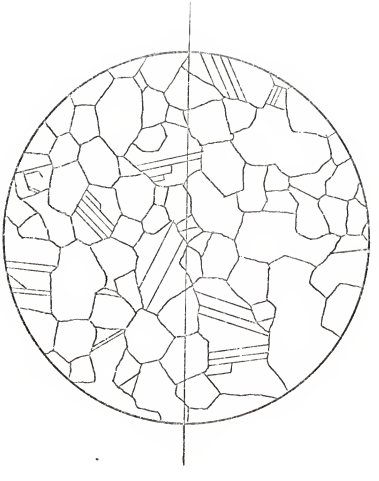

Figure 16. Method of determining the fraction of twinned grains.

Figure 17. A twinned grain in the longitudinal specimen strained 0.6 percent without the appearance of a serration. Polarized light. Magnification 440 times.

Figure 18. Microstructure of the longitudinal specimen strained 1.4 percent just enough to form a serration. Polarized light. Magnification 1000 times.

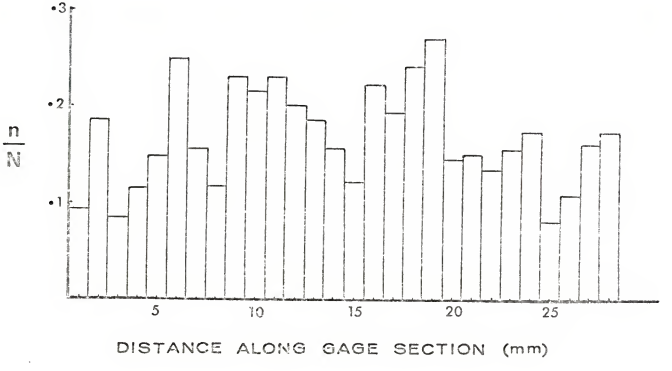

Figure 19. Variation of the fraction of twinned grains along the gage section of the longitudinal specimen deformed to the point where only a single serration appeared.

the variation of the fraction of twinned grains, n/N, along the gage length. It varies between 0.08 and 0.27, with an average of about 0.17. In a given grain of this specimen, the twins are larger and more numerous than in the specimen without a serration. Also there is a higher percentage of $\{11\bar{2}2\}$ twins. Thus when the strain is about doubled and a serration occurs, the volume fraction of twins increases by more than five times. Thus it is seen that though twinning is not as important in a longitudinal as in a transverse specimen, twinning is observed in this type of specimen both before and after the first serration.

Figure 20 shows the microstructure of a transverse specimen strained 0.86 percent. As expected there are many more twinned grains in this specimen than in the longitudinal specimen strained to 1.4 percent, shown in Fig. 18. The twins are mostly $\{11\bar{2}1\}$, in agreement with the transverse specimen texture.

Consider next the effect of large strains. The microstructure of a longitudinal specimen near the point of specimen fracture is shown in Fig. 21. The region is heavily twinned and it is difficult to distinguish between twins and matrix. Due to the heavy distortion, it is equally difficult to distinguish between the various twinning modes. Away from the region of fracture, the $\{11\bar{2}2\}$ type twin, shown in Fig. 22, was found in many grains, as expected in the present longitudinal specimen. Figure 23 shows the microstructure near the fracture in the transverse specimen. Here again the twin density is much larger than in the longitudinal specimen.

Figure 20. Microstructure of the transverse specimen strained 0.86 percent. Polarized light. Magnification 400 times.

Figure 21. Microstructure of the longitudinal specimen near fracture. Polarized light. Magnification 400 times.

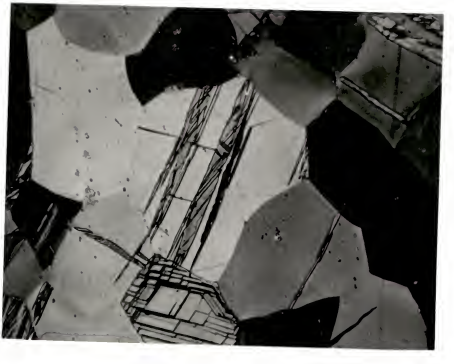

Figure 22. $\{11\bar{2}2\}$ twins in the longitudinal specimen. Polarized light. Magnification 800 times.

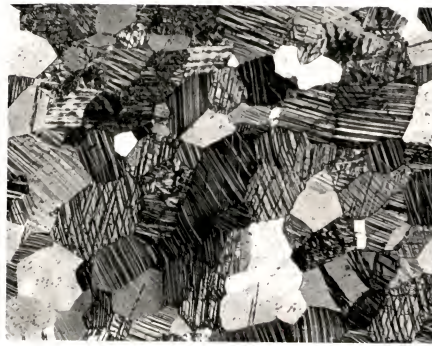

Figure 23. Microstructure of the transverse specimen near fracture. Polarized light. Magnification 400 times.

3.1.5. Strain Distribution

Figure 24 shows the strain distribution along the gage length of two longitudinal specimens deformed to fracture at 4.2°K and 77°K respectively. The original diameter of both specimens was about 0.13 in., as indicated by the upper curve in both halves of this figure. After fracture, the specimen cross sections became slightly elliptical due to a small strain anisotropy in the cross section. For this reason, the diameter, as measured along both the major and minor axes of the ellipse, is recorded in each part of the figure. Now compare the curves given in the bottom part of the figure for the same material at 77°K. At 77°K, zirconium deforms smoothly and continuously to fracture without serrations in the load-elongation curve. The strain distribution appears to be similar at the two temperatures, whether the deformation is accompanied by serrations or not.

3.2. Deformation at Higher Temperatures

3.2.1. Stress-Strain Curves

The conventional stress-strain curves of coarse grained zirconium for the strain rate, 1.3×10^{-2} sec^{-1}, are shown in Figs. 25 and 26 for various temperatures from 77°K to 1032°K. From the general shape of the stress-strain curves, it is apparent that the work hardening rate of zirconium is very high at 77°K and decreases steadily with rise in temperature. In a tensile test of a ductile metal like zirconium, after the maximum load is reached, necking starts and the load drops

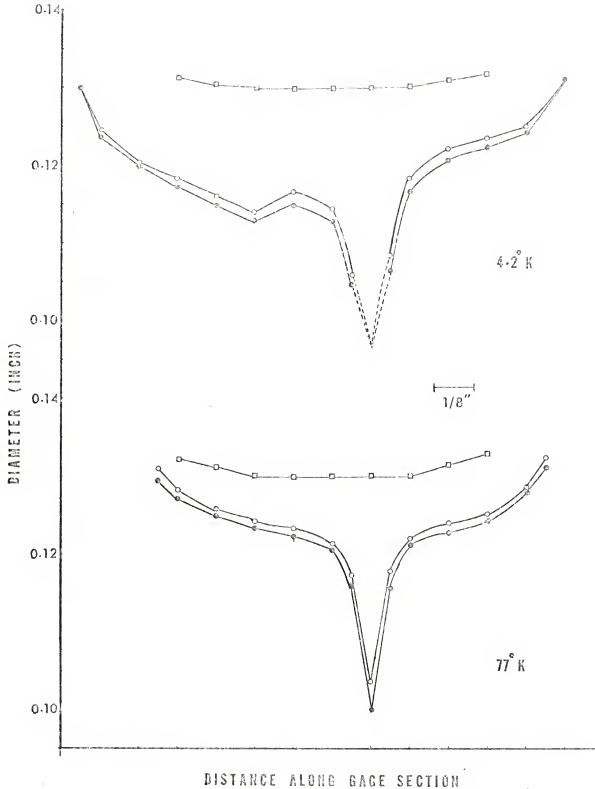

Figure 24. Strain distribution in the longitudinal specimens deformed at 4.2° and 77°K.

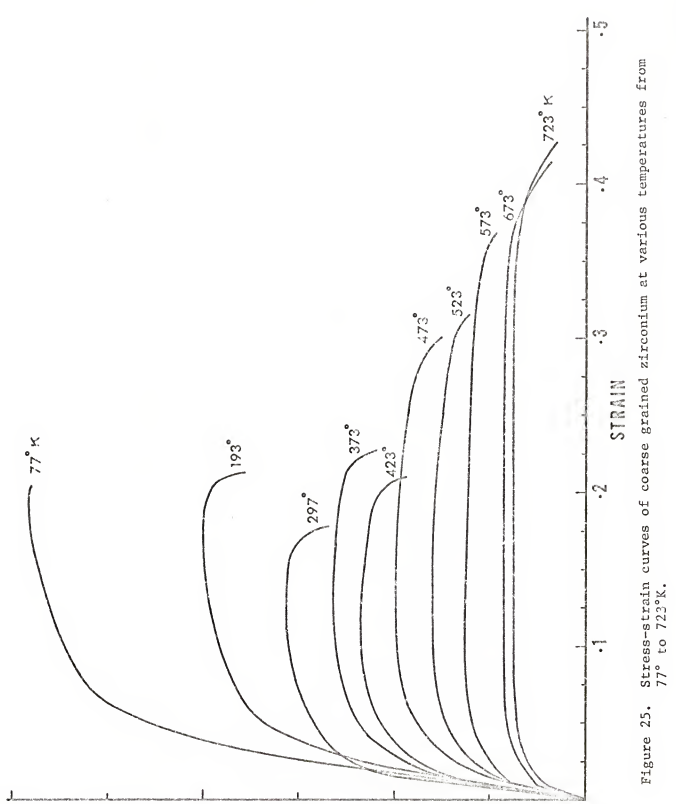

Figure 25. Stress-strain curves of coarse grained zirconium at various temperatures from 77° to 723°K.

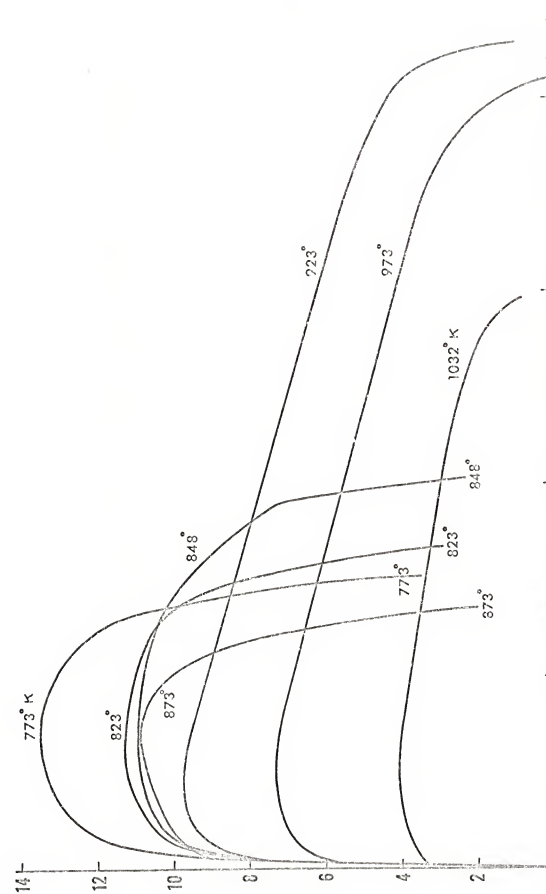

Figure 26. Stress-strain curves of coarse grained zirconium at various temperatures from 773° to 1032°K.

until the specimen fractures. All the strain in the final stages of the test is localized around the neck. Hence the total strain in the specimen consists of two components, the uniform strain up to the point of necking and the necking strain which is the strain between the ultimate stress and fracture. At 77°K, as soon as the ultimate stress is reached, the metal fails with little necking strain. Hence practically all the strain in the specimen is uniform strain. With increase in temperature, the necking strain increases. However, at 873°K there is a drop in the necking strain but at 923°K the necking strain rises very sharply. The uniform strain, on the other hand, does not alter appreciably with change in temperature. These features are clear in the strain plots shown in Fig. 27.

3.2.2. Hardening Peaks

The true flow stresses of zirconium corresponding to four strains are plotted as a function of temperature in Figs. 28 and 29 for the two strain rates. The hardening peaks, indicated by arrows, are not as pronounced as the similar peaks observed in 16 μ grain size titanium specimens.[45] The small size of the peaks may be a result of the coarser grain size of the present zirconium specimens. The peaks are easier to see when the flow stress data are plotted on semilogarithmic coordinates. This is done in Figs. 30 through 33 for 0.2 percent, 1 percent, 2 percent and 5 percent strains respectively. In general, the logarithm of the flow stress of zirconium and titanium tends to decrease linearly with increasing temperature.[31,34,45] It has also been observed empirically that positive deviations from these

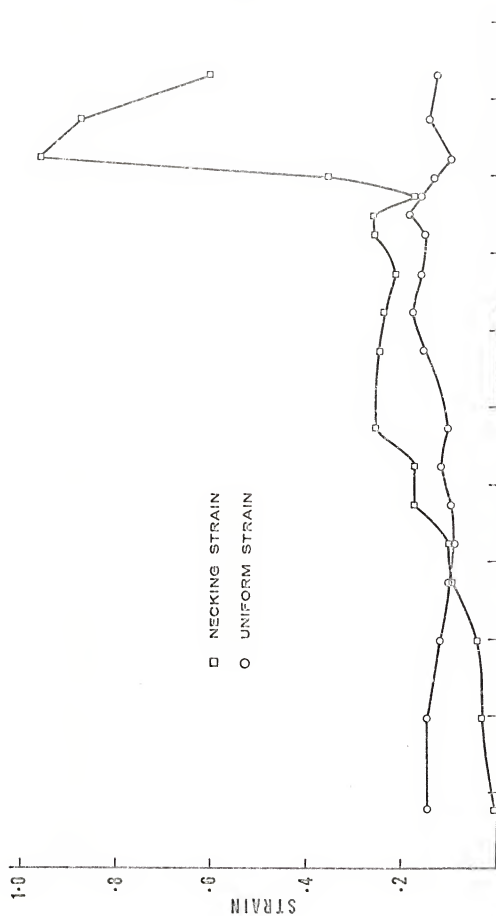

Figure 27. Uniform strain and necking strain versus temperature.

Figure 28. Flow stress of zirconium for various strains versus temperature at a strain rate of 1.3×10^{-2} sec^{-1}.

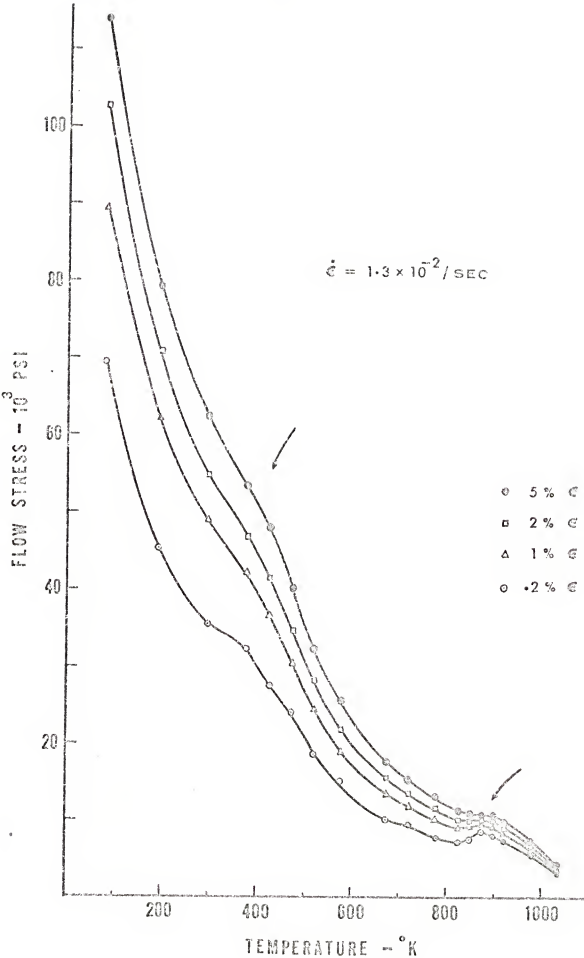
$\dot{\epsilon} = 1{\cdot}3 \times 10^{-2}$/SEC
5 % ε
2 % ε
1 % ε
·2 % ε
FLOW STRESS - 10^3 PSI
100
80
60
40
20
200
400
600
800
1000
TEMPERATURE - °K

Figure 29. Flow stress of zirconium for various strains versus temperature at a strain rate of 1.3×10^{-5} sec^{-1}.

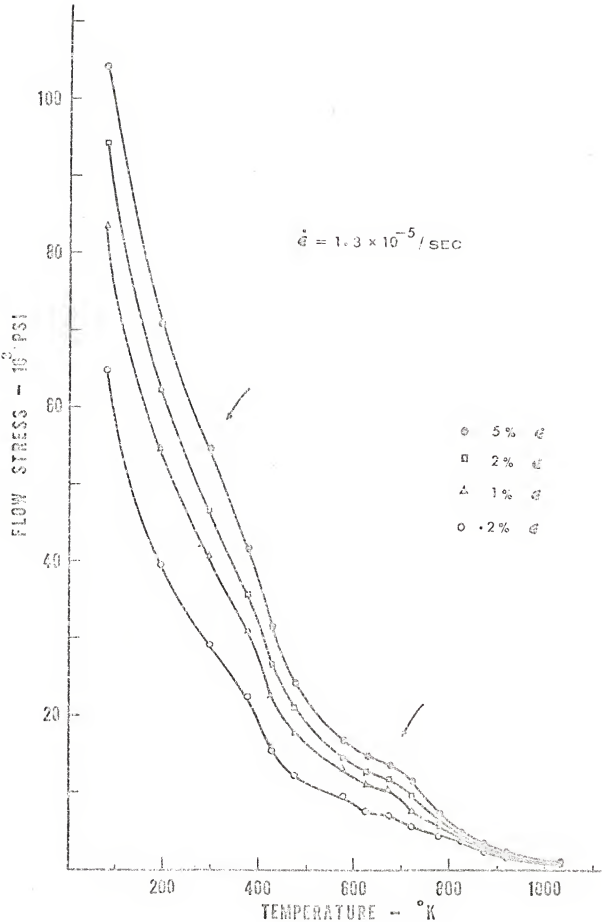
100
80
60
40
20
FLOW STRESS - 10^2 PSI
$\dot{\epsilon} = 1.3 \times 10^{-5}$ / SEC
5 % ϵ
2 % ϵ
1 % ϵ
.2 % ϵ
200
400
600
800
1000
TEMPERATURE - °K

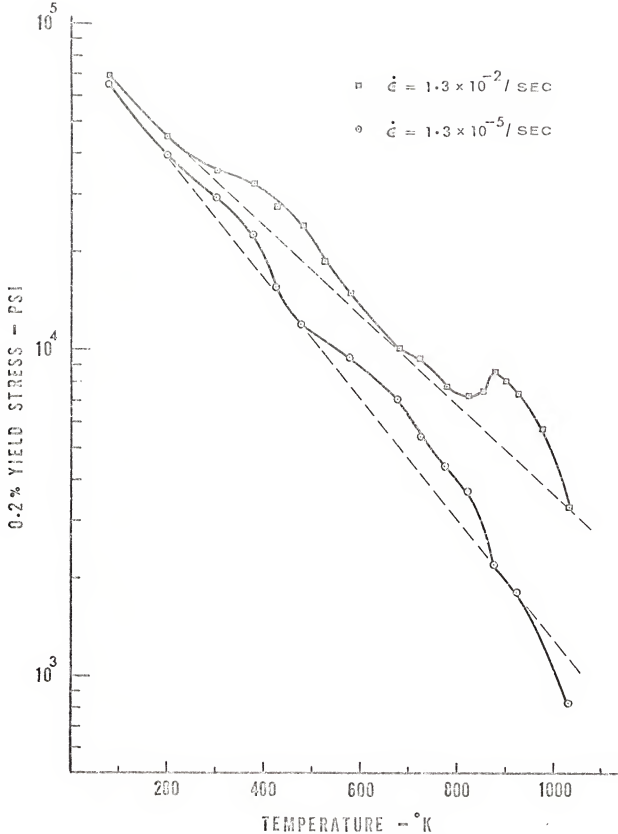

Figure 30. Logarithm of the 0.2 percent yield stress of zirconium as a function of the temperature.

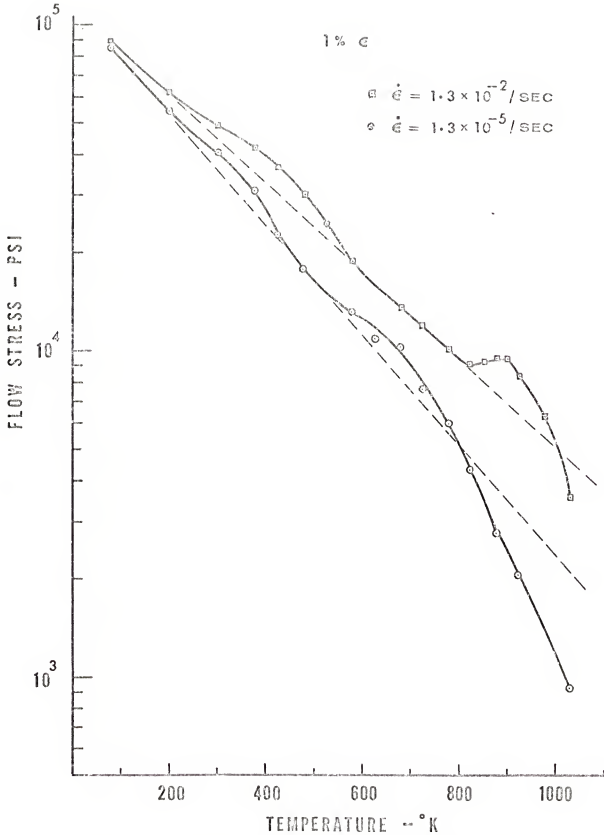

Figure 31. Logarithm of the flow stress of zirconium at 1 percent strain as a function of the temperature.

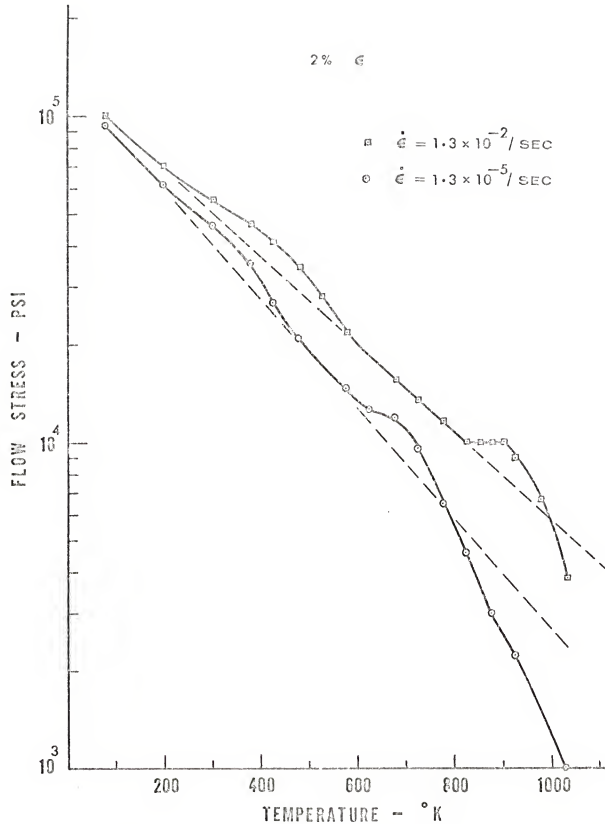

Figure 32. Logarithm of the flow stress of zirconium at 2 percent strain as a function of the temperature.

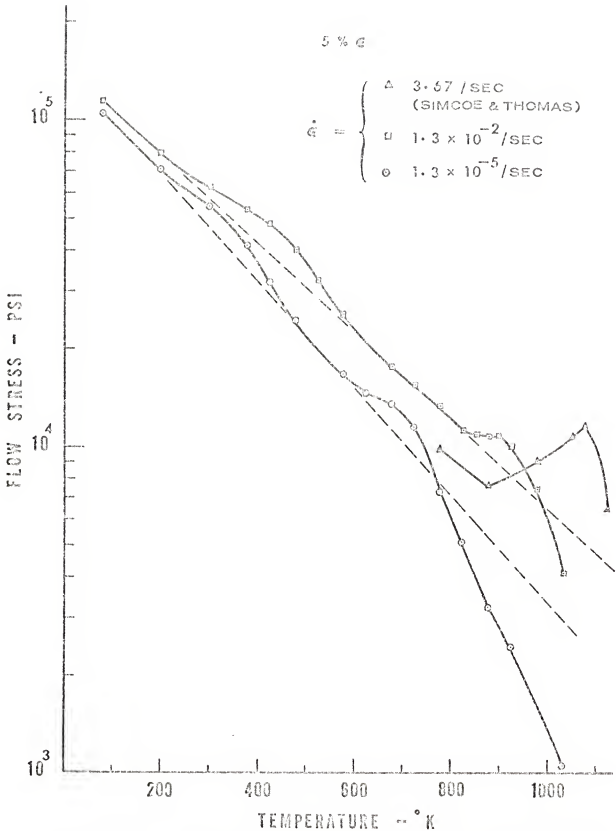

Figure 33. Logarithm of the flow stress of zirconium at 5 percent strain as a function of the temperature.

lines occur in the same temperature ranges where those phenomena normally associated with dynamic strain aging are observed. The negative deviation from the straight lines at very high temperatures can be largely rationalized in terms of the occurrence of recovery and recrystallization in the specimen during deformation. The negative deviation always increased with decreasing strain rate, increasing temperature, and increasing strain. All these factors should promote recovery and recrystallization. It is interesting to note that at the slow strain rate, the specimen deformed at 773°K did not show any sign of recrystallization even at regions of large deformation near the point of fracture. Figure 34 shows the deformed grains in this specimen, whereas the corresponding specimen tested at 823°K showed definite evidence of recrystallization, as shown in Fig. 35; the recrystallized grain size was about 4 μ. At this point, it is not certain whether recrystallization occurred in this specimen during deformation or after the test. However the metallographic study suggests the existence of the conditions for recrystallization in the specimen during deformation, which might have been responsible for the deviation.

At the higher strain rate, as may be seen in Figs. 30 to 33, the hardening peaks fall at 875°K and 425°K, while at the lower strain rate they occur at 675°K and about 300°K respectively. Note that the higher temperature peak is more pronounced than the lower temperature one.

Next consider the high temperature hardening peak, shown in

Figure 34. Deformed grains in a zirconium specimen tested at 773°K. Strain rate 1.3×10^{-5} sec^{-1}. Polarized light. Magnification 50 times. Recrystallization was not observed even at higher magnifications in this specimen whose flow stress at high strain lies almost on the straight line in Fig. 33.

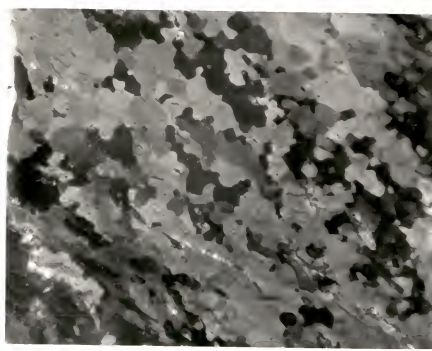

Figure 35. Recrystallization in a zirconium specimen deformed to fracture at 823°K. Strain rate 1.3×10^{-5} sec^{-1}. Polarized light. Magnification 1300 times. The flow stress of this specimen fell well below the straight line in Fig. 33.

Fig. 33. A strain rate change of three orders of magnitude shifts this peak by about 200°. A further increase in strain rate should move this peak to even higher temperatures. In this regard, it is interesting that Simcoe and Thomas[52] obtained a hardening peak in zirconium at 1073°K, using a strain rate equivalent to that employed in hot rolling. This was about 2-1/2 orders of magnitude higher than the faster strain rate of the present work. The present results are thus in reasonable agreement with the location of this peak.

3.2.3. Elongation Minima

Figure 36 shows the total elongation of the zirconium specimens as a function of temperature. Note that at each strain rate the elongation tends to be a minimum at the temperature of the hardening peak. This effect, which is most easily seen at the higher temperature hardening peak, suggests a close association between dynamic strain aging and the elongation minima. The similarity between the curve for the higher strain rate in this figure and that showing the variation of the necking strain with temperature in Fig. 27 indicates that the total elongation value of the specimen is probably controlled by the strain in the neck.

In order to check whether the elongation minima are associated with brittle fracture, the specimens were sectioned and examined metallographically. In the specimens deformed at the temperature near the upper hardening peak, porosity of a type associated with creep and intergranular fracture was found, as shown in Fig. 37. This suggested that the intermediate temperature ductility minimum in metals

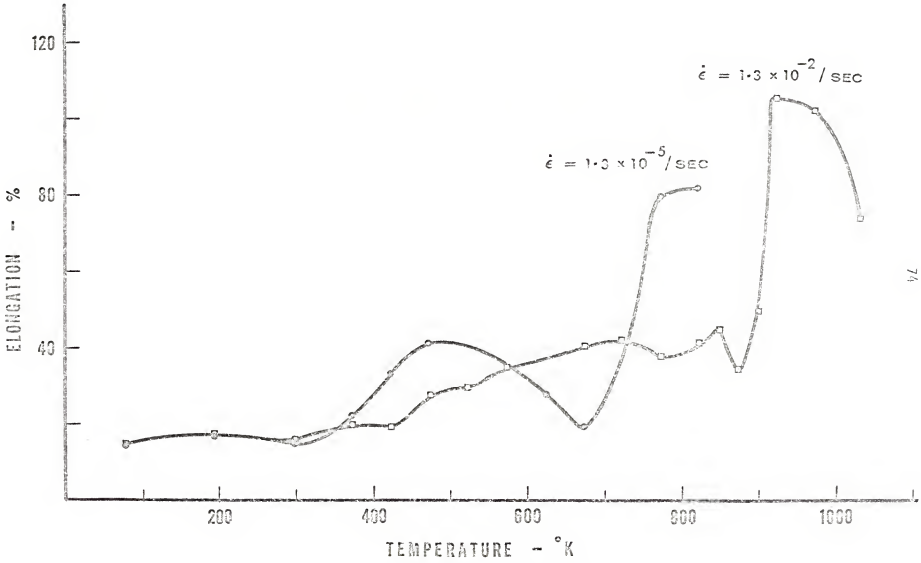

Figure 36. The percentage elongation of zirconium versus the temperature for the two strain rates.

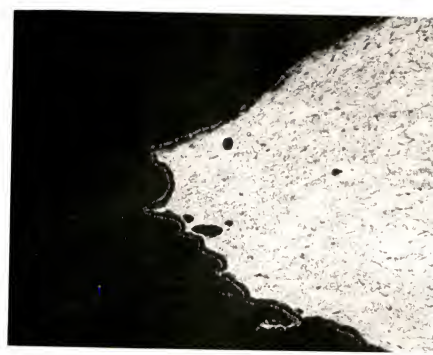

Figure 37. Porosity in a zirconium specimen deformed to fracture under conditions of minimum elongation.

reported by Rhines and Wray[53] may be related to dynamic strain aging. However, porosity was also found, although to a lesser degree, in specimens deformed at other temperatures well above and below the temperature of the hardening peaks.

3.2.4. Reduction in Area

In order to check whether the ductility is really a minimum in the dynamic strain aging region and whether the porosity is associated with brittle fracture, the percentage reduction in area of the specimens was measured at all temperatures. The results are shown in Fig. 38 for both strain rates. It is clear that the reduction in area increases with temperature at both strain rates and there is no minimum in the reduction in area corresponding to the elongation minimum. Furthermore, in the upper dynamic strain aging region, the reduction in area is very large, about 90 percent, indicating a basically ductile fracture. Similar features are implied in the published results on columbium.[40] Thus it is seen that dynamic strain aging conditions reduce the elongation of the metal but not its reduction in area. In other words, in these metals dynamic strain aging is apparently not associated with brittle fracture.

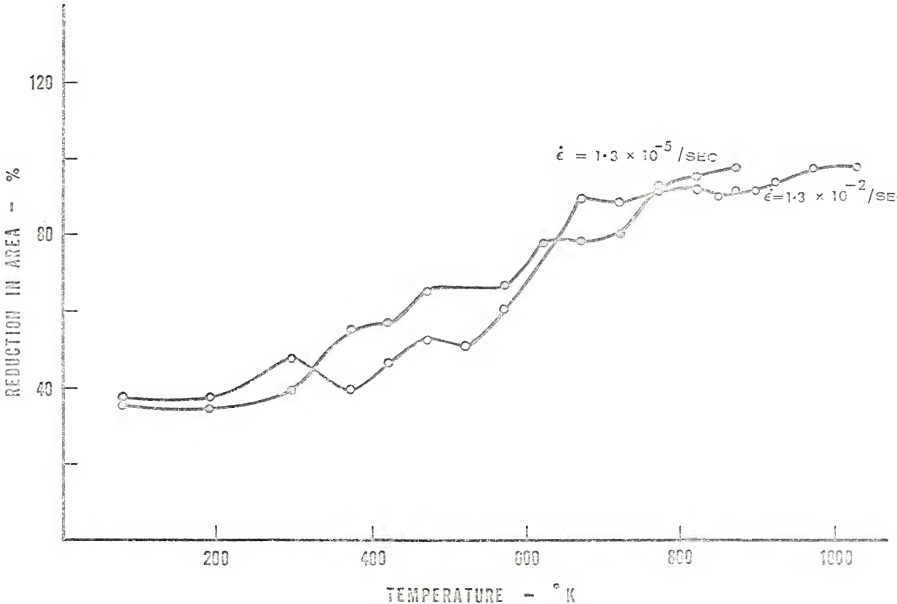

Figure 38. The percentage reduction in area of zirconium versus the temperature for the two strain rates.

CHAPTER IV

DISCUSSION

4.1. Deformation at 4.2°K

4.1.1. Thermal Softening

Deformation in zirconium at 4.2°K is characterized by discontinuous plastic flow. Though it is generally agreed that the load drops during a tensile test near absolute zero are primarily due to thermal softening[10] accompanying localized specimen heating, there are still certain aspects that are not fully explained. For example, Kula and DeFisto[13] have discussed serrated yielding conditions in terms of a balance between strain hardening and geometrical as well as thermal softening. In a specimen undergoing uniform deformation, the load F is given by

$$F = \sigma A \tag{14}$$

where σ is the true stress and A the instantaneous cross sectional area. The incremental load change dF as the specimen is strained by an amount $d\varepsilon$ is given by

$$dF = \sigma dA + A d\sigma \tag{15}$$

where $Ad\sigma$ is the load increment due to strain hardening and σdA is the load decrement due to decrease in specimen cross section. The flow stress σ, unless complicated by structural changes in the metal, generally depends on strain ε, strain rate $\dot{\varepsilon}$, and temperature T so that equation 15 can be written as

$$dF = \sigma dA + A\left[\left(\frac{\partial\sigma}{\partial\varepsilon}\right)_{\dot{\varepsilon},T} d\varepsilon + \left(\frac{\partial\sigma}{\partial\dot{\varepsilon}}\right)_{\varepsilon,T} d\dot{\varepsilon} + \left(\frac{\partial\sigma}{\partial T}\right)_{\varepsilon,\dot{\varepsilon}} dT\right] . \tag{16}$$

Neglecting strain rate effects that are believed to be negligibly small near absolute zero, this equation becomes

$$dF = \sigma dA + A\left[\left(\frac{\partial\sigma}{\partial\varepsilon}\right)_{\dot{\varepsilon},T} d\varepsilon + \left(\frac{\partial\sigma}{\partial T}\right)_{\varepsilon,\dot{\varepsilon}} dT\right] . \tag{17}$$

From the definition of true strain,

$$dA = -Ad\varepsilon . \tag{18}$$

Substituting for dA in equation 16, one gets

$$dF = A\cdot d\varepsilon\left[\left(\frac{\partial\sigma}{\partial\varepsilon}\right)_{\dot{\varepsilon},T} - \sigma + \left(\frac{\partial\sigma}{\partial T}\right)_{\varepsilon,\dot{\varepsilon}} \frac{dT}{d\varepsilon}\right] \tag{19}$$

$$= A\cdot d\varepsilon\left[\left(\frac{\partial\sigma}{\partial\varepsilon}\right)_{\dot{\varepsilon},T} - \sigma + \left(\frac{\partial\sigma}{\partial T}\right)_{\varepsilon,\dot{\varepsilon}} \frac{\alpha\sigma}{\rho c}\right] \tag{20}$$

where $\frac{\partial\sigma}{\partial\varepsilon}$ represents work hardening during continuous deformation, $\frac{\partial\sigma}{\partial T}$ represents the temperature dependence of flow stress, α is the fraction of plastic work converted to heat, ρ the density and c the specific heat of the metal. $-\sigma Ad\varepsilon$ is the geometric softening due to decrease in the cross sectional area of the specimen. $\frac{\alpha\sigma}{\rho c}$ is the heat generated in the specimen.

According to Kula and DeSisto,[13] a load drop will occur when

$$\frac{\partial\sigma}{\partial\varepsilon} - \sigma = \frac{\partial\sigma}{\partial T}\cdot\frac{\alpha\sigma}{\rho c} . \tag{21}$$

For titanium, assuming 0.5 for α, they estimate $\frac{\partial \sigma}{\partial T} \cdot \frac{\alpha \sigma}{\rho c}$ to be -4×10^7 psi which they consider more than enough to ensure a load drop at yielding. However, the yield stress of titanium is 1.26×10^5 psi and the strain hardening rate at yield is 9×10^5 psi per unit strain, so that the quantity $\frac{\partial \sigma}{\partial \varepsilon} - \sigma$ is only 7.74×10^5 psi. This is smaller than the thermal softening term $\frac{\partial \sigma}{\partial T} \cdot \frac{\alpha \sigma}{\rho c}$ by about two orders of magnitude. If the thermal softening term is correctly estimated, this means that a load drop should occur in the microstrain region. However, in Kula and DeSisto's 4.2°K stress-strain curve of titanium, the first load drop appears to have taken place in the plastic region and not in the microstrain region.

In the present case of zirconium, the first load drop did not occur until after a plastic strain of about 1.4 percent in the longitudinal specimen and 4.0 percent in the transverse. At the stress level of the first load drop in the transverse specimen, a similar computation gives -5×10^7 psi for the thermal softening term $\frac{\partial \sigma}{\partial T} \cdot \frac{\alpha \sigma}{\rho c}$, and 1.02×10^5 psi for $\frac{\partial \sigma}{\partial \varepsilon} - \sigma$. This itself shows the inconsistency between the predicted occurrence of the first serration and the experimental observation. There are many other materials such as copper,[11] nickel,[12] K-Monel,[13] cupronickel,[15] lithium,[14] stainless steels,[16] aluminum[10] and 2024 aluminum alloy [20] in which the serrations start only after considerable plastic deformation. These examples imply that, in many cases, Kula and DeSisto's[13] relation does not accurately predict the occurrence of the first load drop.

An important factor neglected by earlier workers, which could

influence the rate of thermal softening, is the heat loss from the specimen to the surroundings. The discrepancy by two orders of magnitude between the values of $\frac{\partial \sigma}{\partial \varepsilon} \cdot \sigma$ and $\frac{\partial \sigma}{\partial T} \cdot \frac{\alpha \sigma}{\rho c}$ suggests that about 99 percent of the heat generated in the specimen is lost and hence not available for thermal softening. In other words, heat is lost at a rate much faster than the rate at which it is accumulated. There can be heat loss by conduction down the specimen to the grips and also by conduction from the specimen to the liquid helium. This latter heat loss is promoted by the agitation produced by the boiling of liquid helium in the Dewar. In order to explain the load drops, it might be postulated that if, for some reason, an insulating film of vapor should form and remain on a portion of the specimen for a sufficient length of time, the reduction in the heat loss from that region might promote an instability and consequent load drop.

4.1.2. Room Temperature Damping Properties

An enhancement in the room temperature damping capacity of zirconium by nucleation of thin $\{11\bar{2}1\}$ twins at low temperatures is believed to be due to stress induced movement of $\{11\bar{2}1\}$ twin boundaries.[8] Reed-Hill, Buchanan and Caldwell[54] have shown that under conditions of small strains, deformation twinning tends to occur with less and less accompanying slip as the temperature is decreased. This implies that twins formed at very low temperatures are surrounded by a matrix which is less distorted than at higher temperatures. As a result, such twin boundaries should be more mobile. The enhanced damping capacity obtained by prestraining at 4.2°K can possibly be explained in this manner.

4.1.3. Role of Twinning in Discontinuous Plastic Flow

The next important aspect to be considered is the possible role of twinning in the formation of serrations. A simple calculation shows that the elongation in a polycrystalline tensile specimen due to one twin is about 3×10^{-9} in., whereas the increase in length associated with a typical load drop is of the order of 4×10^{-3} in., about a million times larger. If the serrations were due to twinning alone, this would imply the formation of more than 10^{6} twins to cause one load drop. In the case of a single crystal where the strain associated with a twin can be large, a load drop might result from an individual twinning event. But it has been shown by Blewitt, Coltman and Redman[11] that copper crystals at 4.2°K deform by pronounced discontinuous slip before twinning starts. This alone indicates that serrations can occur without the need for twinning.

With respect to the present work on zirconium, it should be pointed out that Kula and DeSisto[13] have already observed that in titanium at 4.2°K twinning occurs both before and after the onset of serrations. As a result, they concluded that twinning per se may not be responsible for discontinuous yielding. The present observation of twinning in a longitudinal specimen before and after the first load drop, and the fact that serrations form far more readily in longitudinal specimens than in transverse specimens, further strengthens their conclusion. Furthermore, in the transverse specimen more strain

occurred before the first load drop and between the load drops than in the longitudinal specimen. This is also inconsistent with the concept that the load drops are directly related to twinning. This is because transverse specimens are known to deform readily by twinning even at 77°K,[6] and at small strains (below 1 percent) almost all the strain can be accounted for by twinning.[54] On the other hand, in longitudinal specimens twinning is of much less importance in the plastic flow of the metal and plastic deformation depends much more on slip.

4.1.4. The Work Hardening Rate between Load Drops

One interesting feature of the stress-strain curve of Fig. 13 is that between the load drops in the transverse specimen the work hardening rate is greater than during continuous flow. This is implied by the slope of the load-time chart of Fig. 14(a) in the interval BC. It is believed that this apparently higher work hardening rate is related to the fact that, between load drops, deformation occurs only in a fraction of the gage length. When the gage section is shortened, then for a given crosshead movement the strain in that region is increased, with the result that the apparent strain hardening rate is also increased according to Cottrell and Stokes.[55] Also note that this work hardening rate is not the same in every case (cf. BC, DE, FG). This implies that different lengths of the gage section may undergo deformation between the various load drops. The extent of load drop is also not uniform. This is again probably related to the length of the deforming region. There is some small

correlation between the magnitude of the slope before the load drop and the extent of the load drop. Presumably, the smaller the deforming region, the more localized would be the heat generation and hence the larger would be the temperature rise and the extent of load drop.

An important distinction between transverse and longitudinal specimens is that the amount of plastic deformation between load drops is larger in the former. This difference is probably related to the greater overall work hardening rate in transverse specimens. The larger the work hardening rate, the greater should be the resistance to thermal softening.

4.1.5. Strain Distribution along the Gage Section

In the longitudinal specimen deformed to just beyond the first serration, the high twin density near the center of the gage section, as seen in Fig. 19, is consistent with the assumption that plastic deformation during a load drop occurs in only a fraction of the gage section. The region that deformed first might be expected to strain harden sufficiently so that the next deformation would tend to occur elsewhere. When deformation continues by a series of serrations, localized flow probably tends to occur at a different location each time. Thus in a specimen tested to fracture at 4.2°K, the overall effect should be a rather uniform strain distribution throughout the gage length, just as in a specimen tested at 77°K, where there is no discontinuous flow. In this regard, attention is called to the fact that there is no significant difference in the strain distribution plots of Fig. 24 for specimens deformed at both 4.2°K and 77°K.

4.1.6. Temperature Rise during Load Drops

From the average load during a typical load drop and the extension between load drops, the strain energy converted to heat can be calculated. Such an estimation was made for a typical load drop of 133 lbs which occurred at a load level of 1473 lbs. The temperature rise in the specimen would depend on the volume in which this heat is concentrated. Basinski[10] obtained a reasonable agreement between the observed and calculated load drops, assuming that the heat is generated in a small cylindrical volume whose length was between 1 and 3.3 times the diameter of the specimen. From a plot of the heat capacity data of zirconium[56,57] as a function of temperature, shown in Fig. 39, the maximum temperature rise in the specimen was estimated, assuming that the length of the deforming region was equal to the diameter of the specimen. For the longitudinal specimen, the temperature rise in a typical load drop of 133 lbs was estimated to be about 74°K.

According to Chin, Hosford and Backofen,[20] the discontinuous flow would be arrested as soon as the load level reached a value corresponding to the flow stress at the higher temperature. On this basis, if the temperature in the specimen rose to 78°K, which is close to the temperature of liquid nitrogen, the extent of load drop could be predicted from a comparison of the flow curves of zirconium at liquid helium and liquid nitrogen temperatures. At a strain level equivalent to that of the load drop of 133 lbs which occurred in the 4.2°K test, the predicted load drop is, however, 248 lbs. This discrepancy may be due to two reasons. The length of the deforming region is probably

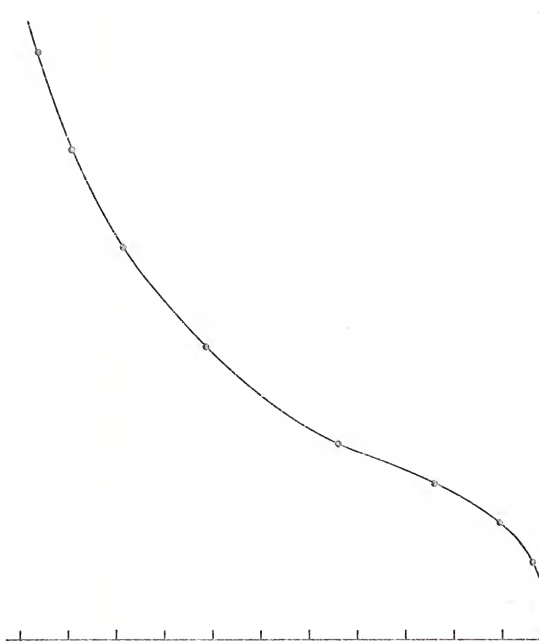

Figure 39. Variation of the specific heat of zirconium with temperature.

more than the assumed value of 0.125 in., in which case the temperature rise might be less than 74°K. Also there might be some heat loss even during the load drop, resulting in a smaller temperature rise and hence a smaller load drop. In the former case, the temperature rise corresponding to different assumed lengths of the deforming region, estimated from Fig. 39, is given in Table 4.

4.1.7. Effect of Recooling on the Shape of the Load-Time Curve

At the end of the load drop the specimen is at its maximum temperature. As may be seen in the load-time chart of Fig. 14, a period of about 15 to 20 seconds is required to regain the load level at which the next load drop occurs. This time interval is much larger than the time taken for the load drop, which, according to Basinski,[10] is about 10^{-4} sec. During this period the specimen undergoes thermal contraction as it cools from about 78°K to 4.2°K. From the thermal expansion data of zirconium due to Cowan et al.,[58] shown in Fig. 40, this contraction was estimated to be 7×10^{-6} in. Also there is an increase in the elastic modulus of the metal during cooling. This should cause an additional contraction in the specimen, which from Fisher and Renken's[59] elastic stiffness moduli of zirconium, was estimated to be 12×10^{-6} in.

The total specimen contraction from these causes is thus very small and of the order of about 19×10^{-6} in. for an assumed 0.125 in. long deforming region. However, the slope of the Instron load-time chart after a load drop was steeper than the initial elastic deformation line; see Fig. 14. This suggests a larger contraction in the specimen.

TABLE 4

TEMPERATURE RISE IN A TYPICAL LOAD DROP CORRESPONDING TO DIFFERENT ASSUMED LENGTHS OF THE DEFORMING REGION

Assumed Length of Deforming Region (in.)	Fraction of Gage Length	Heat Generated (cal. mol^{-1})	Temperature Rise °K
0.125	0.1	104.4	74
0.25	0.2	52.2	57
0.3125	0.25	41.8	54
0.50	0.4	26.1	48
0.625	0.5	20.9	45.5
0.75	0.6	17.4	43.5
1.00	0.8	13.05	40.5
1.25	1.0	10.4	38

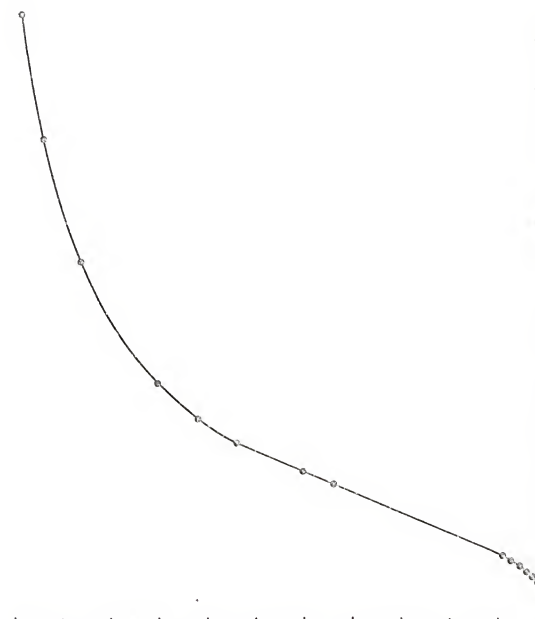

Figure 40. Variation of the coefficient of thermal expansion α of zirconium with temperature.

The initial elastic deformation line had a slope of 48° and the slope after a typical load drop was 50.5°. This steeper slope would correspond to a specimen contraction of about 341 x 10^{-6} in. This calculation takes into account the fact that the deformation after a load drop is partly elastic and partly plastic. Though the contraction depends on the length of the deforming region, it is still very much smaller than that computed from the slope difference on the Instron trace. It is believed that this discrepancy between the computed contraction and the apparent observed contraction is due to errors introduced into the load-time curve by the testing machine itself.

In order to check this assumption, two polycrystalline specimens of titanium were tested at 300°K. In the middle of the test, the specimens were unloaded to an extent comparable to a typical 4.2°K load drop and reloaded. In one test, the data were recorded using load and time as the variables. In the other, a strain gage extensometer was placed on the specimen and load and extension were recorded. These tests showed a steeper reloading slope than the elastic slope on the load-time diagram and no apparent difference in the two slopes of the load-extension curve. This supports the above assumption that the reloading slope at 4.2°K does not truly reflect the contraction in the specimen.

4.2. Dynamic Strain Aging

4.2.1. Dynamic Strengthening

Dynamic strain aging in zirconium is characterized by the

appearance of two peaks in the flow stress-temperature plot. It is believed that they are the result of the interaction of impurity atoms with moving dislocations. Since the hardening peaks are temperature and strain rate dependent, coupling between moving dislocations and diffusing impurity atoms, when the velocities of the dislocations and impurity atoms are roughly comparable, is implied. In other words, at a given strain rate there apparently exists an optimum temperature for interaction between impurity atoms and dislocations.

According to Povolo and Bisogni,[60] there are three internal friction peaks in zirconium due to hydrogen at 144°, 230° and 292°K, determined at a frequency of 1.6 c/sec. These fall within the observed low temperature dynamic strain aging region. Internal friction peaks due to oxygen, nitrogen and carbon in zirconium have not been reported. However, in titanium, internal friction peaks due to these elements have been reported in the high temperature dynamic strain aging region at 700°, 788° and 673°K respectively.[61,62] It is quite probable that similar peaks may also exist in zirconium in the upper dynamic strain aging temperature range. These internal friction results are consistent with an assumption that the low temperature peak in zirconium may be due to dissolved hydrogen and the high temperature peak due to oxygen, nitrogen and/or carbon. The difference between the two regions is probably only one of degree. Recently Lee[63] has recognized the possible contribution of oxygen and carbon in causing strain aging effects in Zircaloy-2.

4.2.2. Strain Rate Sensitivity

The effective strain rate sensitivity of zirconium, calculated from yield stress data at the two strain rates, is plotted as a function of temperature in Fig. 41. The general shape of the curve is quite similar to that obtained by Ramaswami and Craig[64] for zirconium, and Monteiro et al.[37] and Orava et al.[25] for titanium. In general, the strain rate sensitivity tends to increase more or less linearly with temperature in a number of metals. When it falls below this straight line, dynamic strain aging phenomena are also observed. Note the tendency for the strain rate sensitivity to be low in both the dynamic strain aging region near 300°K as well as that centered about 675°K. There are many materials in which minimum strain rate sensitivity is found at about the same temperature as the center of the hardening peak or plateau in the flow stress-temperature diagram. For instance, this has been reported in mild steel by Lubahn,[39] from the data of MacGregor and Fisher,[65] in molybdenum, tantalum and vanadium by Pugh,[66,67,68] in vanadium-oxygen alloys by Bradford and Carlson,[69] in titanium by Orava et al.[25] and Monteiro et al.,[37] and in zirconium-oxygen alloys by Mills and Craig.[70] The regions of abnormally low strain rate sensitivity in Fig. 41 can be explained in terms of the tendency for the temperature corresponding to the hardening peaks to shift with a change in strain rate. This is illustrated in Fig. 42 where the variation of the flow stress with temperature is plotted schematically for two strain rates. Let us, for example, consider the higher temperature dynamic strain aging region. At temperature T_4 the two curves are close to each

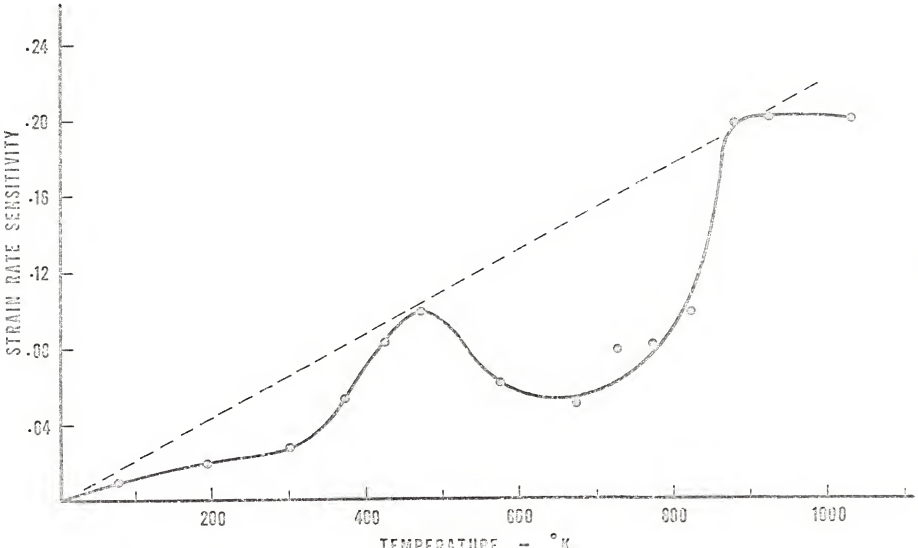

Figure 41. The effective strain rate sensitivity of zirconium as a function of the temperature.

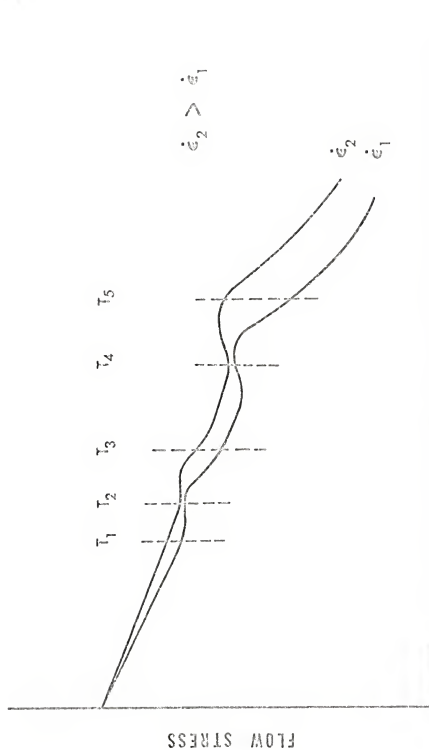

Figure 42. Schematic plot of the temperature dependence of the flow stress of a metal at two strain rates.

other, implying a very small effective strain rate sensitivity. Above and below this temperature, i.e. at T_5 and T_3, the curves diverge, suggesting an increase in strain rate sensitivity. Thus one is able to rationalize the strain rate sensitivity minimum at 675°K, shown in Fig. 41. The other minimum at about 300°K can also be explained in the same manner. It should be pointed out that the exact temperature of the minimum strain rate sensitivity depends on the choice of strain rates. With a different choice of strain rates, a different temperature should be obtained for the minimum effective strain rate sensitivity. This is because the hardening peak falls at a different temperature at each strain rate.

4.2.3. Elongation Minima

In the dynamic strain aging region, elongation minima are observed which are not accompanied by corresponding minima in the reduction in area. This implies that the elongation minima are associated with an increased tendency towards neck formation. This is reflected in the drop in the necking strain (strain between ultimate stress and fracture) in the upper dynamic strain aging region shown in Fig. 27. When necking begins it is normally assumed that the increase in stress due to the reduction in specimen cross section area balances the corresponding increase in strength of the material due to strain hardening. However, in addition to these factors, when a neck forms the effective length of the gage section is also markedly decreased. This means that the strain rate in the necked region is forced to increase. If the strain rate sensitivity is high then the increase in

strain rate may increase the resistance of the metal to flow in the neck sufficiently so that deformation tends to occur elsewhere. On the other hand, this does not happen if the strain rate sensitivity is very low or zero, and the concentration of the deformation in the necked region continues, with the result that a sharp neck occurs. Now let us apply these considerations to the case of zirconium in the upper dynamic strain aging interval. With reference to Fig 42, consider a specimen being deformed at the slower strain rate at temperature T_4. At this temperature the effective strain rate sensitivity is a minimum. Therefore, when necking starts, even though there is an increase in strain rate in the necked region, the flow stress should not increase appreciably. Hence necking should continue in the same region and failure without appreciable elongation should occur.

Now consider a slightly higher temperature such as T_5 where the effective strain rate sensitivity is higher. Here strain rate hardening should take place, tending to force deformation to occur elsewhere in the specimen. The result should be a reduction in the sharpness of the neck or an increase in the necking strain. These considerations are in good agreement with the zirconium stress-strain curves, shown in Fig. 43 taken from the set of curves in Fig. 26, corresponding to the two temperatures 873°K and 923°K and a strain rate 1.3×10^{-2} sec^{-1}. At this strain rate, 873°K corresponds to a minimum effective strain rate sensitivity, while 923°K corresponds to a strain rate sensitivity that is considerably larger. Note that at

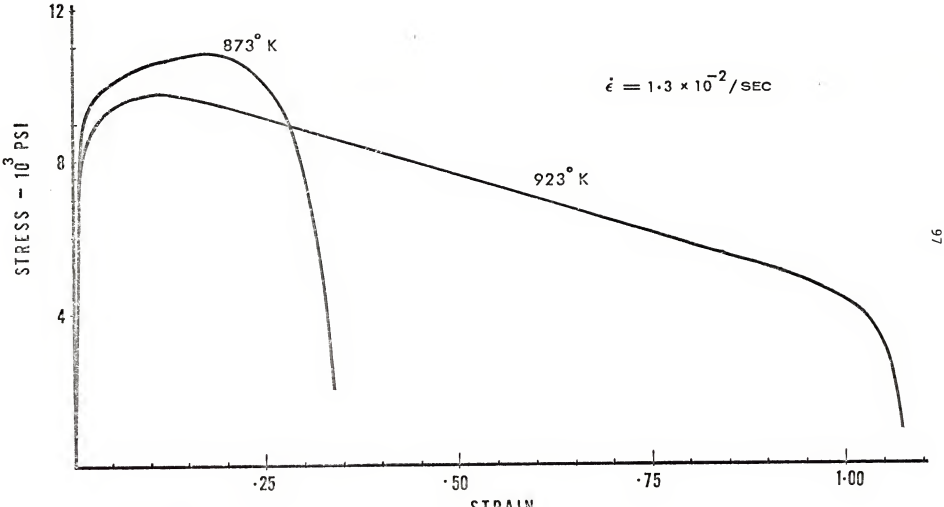

Figure 43. Stress-strain curves of zirconium at 873° and 923°K. Strain rate 1.3×10^{-2} sec^{-1}.

873°K, the maximum stress is reached after 17.4 percent strain, but the specimen fails with a total strain of only 34 percent, whereas at 923°K, even though the maximum stress is reached earlier at 11.8 percent strain, the specimen continues to elongate to about 108 percent before failure. In other words, at 923°K, the necking strain is about 3 times the uniform strain, whereas at 873°K the two strains are comparable. Thus the effective strain rate sensitivity is a factor controlling the elongation of the metal. In this connection it is interesting to note a plot from Woodford's[71] summary, shown in Fig. 44, relating the strain rate sensitivity to the percentage elongation for a variety of materials under different testing conditions. The increase in elongation with increase in strain rate sensitivity over a very wide range is significant. In the present work on zirconium, the temperature dependence of the elongation with a minimum in the dynamic strain aging region is in agreement with this point of view. The present results are also in excellent agreement with the interpretation of the role of strain rate sensitivity in superplasticity by Backofen, Turner and Avery.[72]

4.2.4. Abnormalities in Work Hardening

Monteiro, Santhanam and Reed-Hill[37] have found abnormal work hardening rates in the dynamic strain aging region of commercial titanium of 16 μ grain size. In this material, around 675°K, a slower strain rate produced a greater work hardening rate and a faster strain rate resulted in a smaller work hardening. This has been explained in terms of total dislocation multiplication at slower rates and increase in the mobile dislocation density at faster rates of deformation.

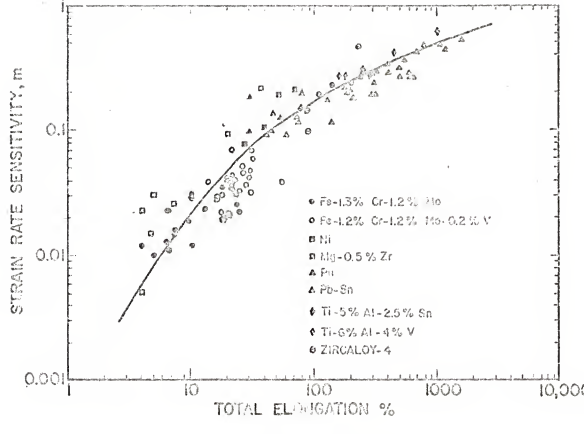

Figure 44. Correlation between strain rate sensitivity and total elongation for a variety of materials.*

(* D. A. Woodford, Trans. ASM, 1969, vol. 62, p. 292)

It was felt desirable to check whether this abnormal work hardening is also true of zirconium. Conventionally the work hardening rate is described by the work hardening exponent, η, defined as

$$\eta = \frac{d\ln\sigma}{d\ln\varepsilon} \tag{22}$$

and taken as the slope of the true stress-true strain diagram plotted on double logarithmic coordinates. A linear relationship between the logarithms of the true stress σ and true strain ε would imply a power law of the form

$$\sigma = A\varepsilon^{\eta} \tag{23}$$

where A is a constant. Such plots for the two strain rates used in the present work on zirconium are shown in Figs. 45 and 46. The variation of the work hardening exponent η with temperature is shown in Fig. 47. It may be seen that the power law is apparently obeyed at all temperatures in zirconium. However, as shown by Reed-Hill[73] in the case of titanium, this may be fortuitous.

Figures 45 and 46 imply that the work hardening exponent η determined in the above manner is almost the same at all temperatures except in the dynamic strain aging region where there are abnormalities, though not so pronounced as in fine grained titanium. Also from Fig. 47 one tends to infer that below room temperature the work hardening exponent decreases slightly, which is not true. The shape of the stress-strain diagrams in Fig. 25 indicates very clearly the large work hardening rate at low temperatures. Reed-Hill[73] has demonstrated that the magnitude of the work hardening exponent η determined from

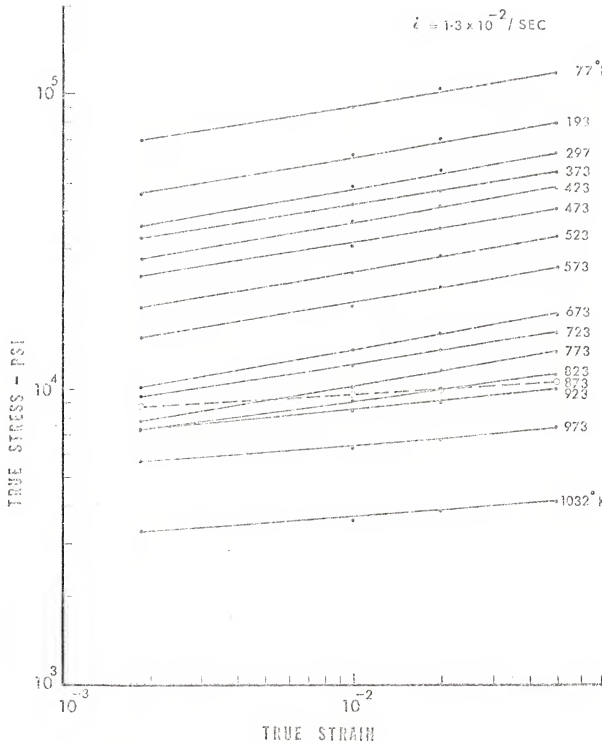

Figure 45. Variation of the logarithm of the true stress with the logarithm of the true strain of zirconium specimens deformed at 1.3×10^{-2} sec^{-1}, at various temperatures.

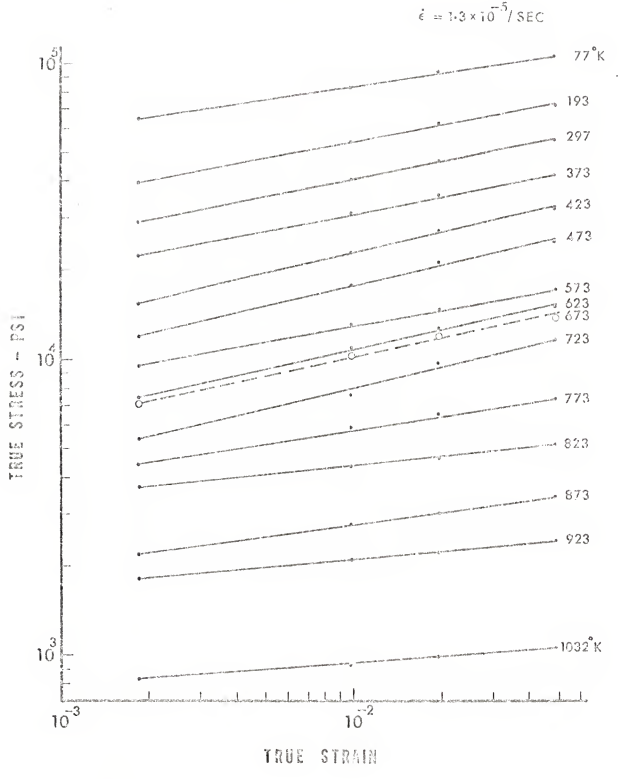

Figure 46. Variation of the logarithm of the true stress with the logarithm of the true strain of zirconium specimens deformed at 1.3×10^{-5} sec^{-1}, at various temperatures.

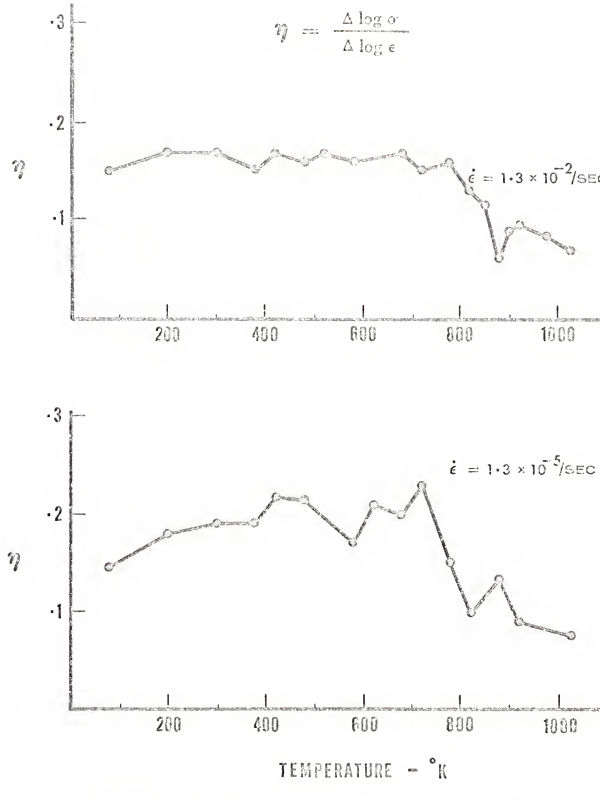

Figure 47. Variation of the work hardening coefficient η of zirconium with temperature.

equation 22 is not a very satisfactory measure of the rate of work hardening in a metal. Since work hardening is related to an increase in the long range component of the flow stress, he has indicated that the strain hardening exponent n of equation 22 would be a more meaningful parameter if it were written

$$\eta = \frac{d\ell n \sigma_{\ell}}{d\ell n \varepsilon} \tag{24}$$

where σ_{ℓ} is the long range component of the flow stress.

In the absence of accurate measurements of σ_{ℓ}, an alternate method of studying the variation of the work hardening rate with temperature was sought. The increase in the true flow stress in the strain interval between 0.2 percent and 5 percent was taken as a relative measure of work hardening. This quantity $\Delta\sigma$, shown in the last columns of Tables 5 and 6 in the Appendix, is plotted against temperature in Fig. 48 for the two strain rates. Note that at each strain rate, $\Delta\sigma$ is very large at low temperatures and decreases steadily with rise in temperature. Consider the dynamic strain aging region. The steady decrease of $\Delta\sigma$ with temperature is interrupted in this region. A dotted line is drawn to indicate the probable variation of $\Delta\sigma$ with temperature, had there been no dynamic strain aging. Dynamic strain aging does cause an increased rate of work hardening. This has been independently verified by dislocation density measurements in iron by Dingley and McLean,[22] Baird and MacKenzie,[74] Brindley and Barnby,[75] and Keh, Nakada and Leslie,[76] in vanadium by Edington and Smallman,[77] and in nickel-hydrogen alloys by Wilcox and Smith.[78] In

Figure 48. Difference between the true flow stresses of zirconium at 5 percent strain and 0.2 percent strain versus temperature.

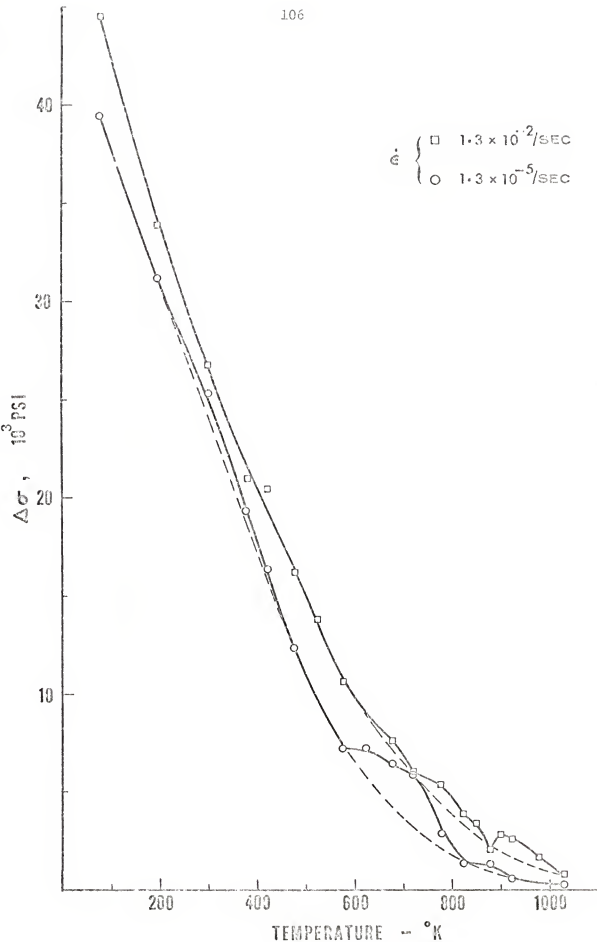
40
30
20
10
$\Delta\sigma$, 10^3 PSI
$\dot{\epsilon}$ □ 1.3×10^{-2}/SEC
○ 1.3×10^{-5}/SEC
200
400
600
800
1000
TEMPERATURE -- °K

the present plot of $\Delta\sigma$ against temperature, such an increase in the work hardening rate in the dynamic strain aging region is apparent. Also in this manner one can clearly see that at the slower strain rate, increase in $\Delta\sigma$ is larger than at the faster strain rate. In materials where the long range component of the flow stress is appreciable, as for example in fine grained metals, these effects can be even larger. More research effort with such materials would be worthwhile.

CHAPTER V

CONCLUSIONS

1. The enhanced ductility of zirconium at 4.2°K could be attributed to the ability of the metal to twin readily at low temperatures.

2. The increased room temperature damping capacity of zirconium produced by prestraining at 4.2°K over that resulting from prestraining at 77°K may be due to the higher mobility of the $\{11\bar{2}1\}$ twin boundaries formed at the lower temperature, because of less distortion in the surrounding matrix.

3. The present study of the discontinuous plastic flow in polycrystalline zirconium confirms the earlier observation of Kula and DeSisto that the cause for serrated flow at 4.2°K may not be twinning per se.

4. During plastic deformation between load drops in the transverse specimen, there is an apparent increase in the work hardening rate, in agreement with the concept that the deformation during a load drop is localized. The region of localized flow is probably different for each serration. As a result, the strain distribution in a specimen tested to fracture at 4.2°K appears to be as uniform as that in a test made at 77°K where the flow is continuous throughout the test.

5. The larger amount of plastic deformation between serrations in the transverse specimen than in the longitudinal specimen is in agreement with the higher work hardening rate in the former.

6. The observation that load drop starts after considerable plastic deformation and not in the microstrain region, as implied by Kula and DeFisto's relation, can be explained by postulating that this is a result of heat loss from the specimen to the surroundings.

7. The temperature rise in a small volume of the specimen during a load drop was estimated to be 74°K. However, the extent of the load drop as a result of this temperature rise is less than that computed from the temperature dependence of the flow stress of the metal. This suggests that an appreciable fraction of the gage length is involved in a load drop.

8. Concurrent with the cooling of the locally heated specimen after each load drop, there is a contraction in the specimen associated with the temperature drop and increase of the elastic modulus. These contractions, however, are very small.

9. In the study of the plastic behavior of coarse grained zirconium over the temperature range, 77°K to 1032°K, two hardening peaks have been observed in the flow stress-temperature diagrams. These peaks are characteristic of dynamic strain aging. The low temperature peak is probably due to interactions between dislocations and hydrogen atoms, and the high temperature peak due to oxygen, nitrogen and/or carbon.

10. The hardening peaks are strain rate dependent, shifting to higher temperatures with increase in strain rate.

11. At the temperature of the center of the peak, the tensile elongation of zirconium tends to be a minimum at each strain rate.

12. The reduction in area, however, is independent of dynamic strain aging. In fact, it is quite large in the upper dynamic strain aging region, indicating ductile fracture.

13. The observed variation of the effective strain rate sensitivity with temperature, with a pronounced minimum at 675°K, is a direct consequence of the shift in the hardening peak temperature with changes in strain rate. The exact temperature of the minimum effective strain rate sensitivity depends on the choice of strain rates.

14. The prevailing strain rate sensitivity which is a minimum under dynamic strain aging conditions leads to minimum elongation in the dynamic strain aging region.

15. Beyond the dynamic strain aging region, the effective strain rate sensitivity can be large and can lead to large elongations.

16. Abnormalities in the work hardening rate are observed in the dynamic strain aging region. These are, however, not so pronounced as in fine grained titanium.

APPENDIX

TABLE 5

TRUE FLOW STRESS OF ZIRCONIUM AT VARIOUS TEMPERATURES AT THE STRAIN RATE 1.3×10^{-2} SEC^{-1}

Temperature	True Flow Stress σ (psi)				$\Delta\sigma = \sigma_{5\%\ \varepsilon} - \sigma_{.2\%\ \varepsilon}$
(°K)	0.2% ε	1% ε	2% ε	5% ε	(psi)
77	69,470	89,380	102,750	114,080	44,610
193	45,390	62,300	70,790	79,280	33,890
297	35,620	49,100	54,810	62,450	26,830
373	32,490	42,150	46,880	53,520	21,030
423	27,550	36,830	41,480	48,020	20,470
473	24,100	30,590	34,830	40,300	16,200
523	18,690	24,590	28,350	32,620	13,930
573	14,960	18,980	21,920	25,620	10,660
673	10,100	13,530	15,540	17,770	7,670
723	9,450	12,100	13,620	15,510	6,060
773	7,830	10,230	11,660	13,300	5,470
823	7,320	9,150	10,080	11,210	3,890
848	7,460	9,270	10,050	10,940	3,480
873	8,710	9,570	9,950	10,670	1,960
898	8,090	9,450	10,060	10,930	2,840
923	7,360	8,390	9,040	10,040	2,680
973	5,700	6,260	6,750	7,470	1,770
1032	3,310	3,590	3,840	4,160	850

TABLE 6

TRUE FLOW STRESS OF ZIRCONIUM AT VARIOUS TEMPERATURES AT THE STRAIN RATE 1.3×10^{-5} SEC^{-1}

Temperature (°K)	True Flow Stress σ (psi)				$\Delta\sigma = \sigma_{5\%\ \varepsilon} - \sigma_{.2\%\ \varepsilon}$ (psi)
	0.2% ε	1% ε	2% ε	5% ε	
77	64,780	83,630	94,200	104,330	39,550
193	39,520	54,740	62,140	70,790	31,270
297	29,250	40,790	46,590	54,660	25,410
373	22,400	31,060	35,720	41,710	19,310
423	15,390	22,820	26,880	31.820	16,430
473	12,110	17,920	21,090	24,490	12,380
573	9,630	13,140	14,740	16,880	7,250
623	7,450	10,970	12,660	14,770	7,320
673	7,140	10,440	11,960	13,620	6,480
723	5,430	7,620	9,620	11,550	6,120
773	4,440	5,950	6,530	7,330	2,890
823	3,700	4,340	4,590	5,120	1,420
873	2,200	2,760	2,990	3,430	1,230
923	1,820	2,080	2,220	2,440	620
1032	822	931	993	1,053	231

BIBLIOGRAPHY

1. E. J. Rapperport, "Deformation Processes in Zirconium," Acta Met., 1955, vol. 3, p. 208.

2. E. J. Rapperport, "Room Temperature Deformation Processes in Zirconium," Acta Met., 1959, vol. 7, pp. 254-60.

3. E. J. Rapperport and C. S. Hartley, "Deformation Modes of Zirconium at 77°, 575°, and 1075°K," Trans. Met. Soc. AIME, 1960, vol. 218, pp. 869-77.

4. J. L. Martin and R. E. Reed-Hill, "A Study of Basal Slip Kink Bands in Polycrystalline Zirconium," Trans. Met. Soc. AIME, 1964, vol. 230, pp. 780-5.

5. D. H. Baldwin and R. E. Reed-Hill, "Some Observations of the Deformation Modes of Polycrystalline Hafnium and Zirconium," Trans. Met. Soc. AIME, 1965, vol. 233, pp. 248-9.

6. R. E. Reed-Hill, "Role of Deformation Twinning in the Plastic Deformation of a Polycrystalline Anisotropic Metal," Deformation Twinning, pp. 295-320, Gordon and Breach Science Publishers, New York, 1964.

7. R. E. Reed-Hill and E. P. Dahlberg, "Some Effects of Prestrain at 77°K on the Mechanical Properties of Zirconium at Room Temperature," Electrochemical Technology, 1966, vol. 4, pp. 303-7.

8. R. E. Reed-Hill, E. P. Dahlberg and W. A. Slippy, Jr., "Some Anelastic Effects in Zirconium at Room Temperature Resulting from Prestrain at 77°K," Trans. Met. Soc. AIME, 1965, vol. 233, pp. 1766-71.

9. H. M. Rosenberg, "Research on the Mechanical Properties of Metals at Liquid Helium Temperatures," Metallurgical Reviews, 1958, vol. 3, pp. 357-79.

10. Z. S. Basinski, "The Instability of Plastic Flow of Metals at Very Low Temperatures," Proc. Royal Soc. London, 1957, Ser. A, vol. 240, pp. 229-42.

11. T. H. Blewitt, R. R. Coltman and J. K. Redman, "Low-Temperature Deformation of Copper Single Crystals," J. Appl. Phys., 1957, vol. 28, pp. 651-60.

12. E. T. Wessel, "Some Exploratory Observations of the Tensile Properties of Metals at Very Low Temperatures," Trans. ASM, 1957, vol. 49, pp. 149-72.

13. E. B. Kula and T. S. DeSisto, "Plastic Behavior of Metals at Cryogenic Temperatures," Behavior of Materials at Cryogenic Temperatures, pp. 3-31, ASTM Spec. Tech. Publ. 387, Amer. Soc. Testing Materials, 1966.

14. D. Hull and H. M. Rosenberg, "The Deformation of Lithium, Sodium and Potassium at Low Temperatures: Tensile and Resistivity Experiments," Phil. Mag., 1959, vol. 4, pp. 303-15.

15. J. C. Erdman and J. A. Jahoda, "Calorimetry of Instantaneous Heat Sources Arising from Plastic Tensile Deformation at Low Temperatures," Boeing Scientific Research Laboratories Document DI-82-0311, October 1963, Seattle, Washington.

16. S. C. Collins, F. D. Ezekiel, O. W. Sepp and J. W. Rizika, "The Strength of Certain Stainless and Carbon Steels at Low Temperatures," Proc. ASTM, 1956, vol. 56, pp. 687-703.

17. C. V. Uzhik, "Strength and Ductility of Metals at Low and Extremely Low Temperatures," Izvestiya Akademi Nauk, USSR, OTN, 1955, No. 1, pp. 56-7.

18. G. W. Powell, E. R. Marshall and W. A. Backofen, Trans. ASM, 1958, vol. 50, pp. 478-97.

19. C. Zener and J. H. Hollomon, "Effect of Strain Rate upon Plastic Flow of Steel," J. Appl. Phys., 1944, vol. 15, pp. 22-32.

20. G. Y. Chin, W. F. Hosford, Jr., and W. A. Backofen, "Influence of the Mechanical Loading System on Low-Temperature Plastic Instability," Trans. Met. Soc. AIME, 1964, vol. 230, pp. 1043-8.

21. A. Seeger, "The Mechanism of Glide and Work Hardening in Face-Centered Cubic and Hexagonal Close-Packed Metals," Dislocations and Mechanical Properties of Crystals, pp. 243-329, John Wiley and Sons, New York, 1957.

22. D. J. Dingley and D. McLean, "Components of the Flow Stress of Iron," Acta Met., 1967, vol. 15, pp. 885-901.

23. W. G. Johnston, "Yield Points and Delay Times in Single Crystals," J. Appl. Phys., 1962, vol. 33, pp. 2716-30.

24. R. E. Reed-Hill, "An Analysis of the Components of the Flow Stress in Titanium," Technical Report to the Air Force Materials Laboratories, Wright-Patterson Air Force Base, November 8, 1967.

25. R. N. Orava, G. Stone and H. Conrad, "The Effects of Temperature and Strain Rate on the Yield and Flow Stresses of α-Titanium," Trans. ASM, 1966, vol. 59, pp. 171-84.

26. E. D. Levine, "Deformation Mechanisms in Titanium at Low Temperatures," Trans. Met. Soc. AIME, 1966, vol. 236, pp. 1558-65.

27. H. Conrad, S. Feuerstein and L. A. Rice, "Work-Hardening Model for the Effect of Grain Size on the Flow Stress of Niobium Strained by Rolling," Trans. Japan. Inst. Metals, 1968, vol. 9, Supplement, pp. 481-7.

28. D. Weinstein, "Yield Point Occurrence in Polycrystalline Alpha-Zirconium," Electrochemical Technology, 1966, vol. 4, pp. 507-12.

29. G. T. Hahn, "A Model for Yielding with Special Reference to the Yield-Point Phenomena of Iron and Related BCC Metals," Acta Met., 1962, vol. 10, pp. 727-38.

30. R. P. Carreker, Jr., "Plastic Flow of Platinum Wires," J. Appl. Phys., 1950, vol. 21, pp. 1289-96.

31. D. H. Baldwin and R. E. Reed-Hill, "Some Effects of Oxygen on the Tensile Deformation of Polycrystalline Zirconium," Trans. Met. Soc. AIME, 1968, vol. 242, pp. 661-9.

32. T. Yokobori, "The Cottrell-Bilby Theory of Yielding of Iron," Phys. Rev., 1952, vol. 88, p. 1423.

33. N. J. Petch, "The Ductile-Brittle Transition in the Fracture of α-Iron: I," Phil. Mag., 1958, vol. 1, pp. 1089-97.

34. R. J. Wasilewski, "On Discontinuous Yield and Plastic Flow in α-Titanium," Trans. ASM, 1963, vol. 56, pp. 221-35.

35. C. E. Coleman and D. Hardie, "Grain-Size-Dependence in the Flow and Fracture of Alpha-Zirconium," J. Inst. Metals, 1966, vol. 94, pp. 387-91.

36. W. G. Johnston and J. J. Gilman, "Dislocation Velocities, Dislocation Densities, and Plastic Flow in Lithium Fluoride Crystals," J. Appl. Phys., 1959, vol. 30, pp. 129-44.

37. S. N. Monteiro, A. T. Santhanam and R. E. Reed-Hill, "Athermal Plastic Deformation in Commercial Purity Titanium," International Conference on Titanium, London, May 1968.

38. A. H. Cottrell, Dislocations and Plastic Flow in Crystals, Oxford University Press, London, 1953.

39. J. D. Lubahn, "Strain Aging Effects," Trans. ASM, 1952, vol. 44, pp. 643-64.

40. E. T. Wessel, L. L. France and R. T. Begley, "The Flow and Fracture Characteristics of Electron-Beam-Melted Columbium," Columbium Metallurgy, pp. 459-502, Interscience Publishers, New York, 1961.

41. A. Portevin and F. Le Chatelier, "On a Phenomenon Observed Concurrent with Transformation during the Tensile Testing of Alloys," Compt. Rend., 1923, vol. 176, pp. 507-10.

42. M. J. Manjoine, "Influence of Rate of Strain and Temperature on Yield Stresses of Mild Steel," Trans. ASME, 1944, vol. 66, pp. A211-8.

43. A. Nadai and M. J. Manjoine, "High-Speed Tension Tests at Elevated Temperatures - Parts II and III," Trans. ASME, 1941, vol. 63, pp. A77-91.

44. J. D. Baird and A. Jamieson, "Effects of Manganese and Nitrogen on the Tensile Properties of Iron in the Range 20-600°C," J. Iron and Steel Inst., 1966, vol. 204, pp. 793-803.

45. S. N. Monteiro, A. T. Santhanam and R. E. Reed-Hill, June 1969, Department of Metallurgical and Materials Engineering, University of Florida, Gainesville, Florida.

46. W. S. Owen and M. J. Roberts, "Dynamic Aging Effects in Ferrous Martensite," Trans. Japan Inst. Metals, 1968, vol. 9, Supplement, pp. 911-8.

47. P. L. Rittenhouse and M. L. Picklesimer, "Metallurgy of Zircaloy-2. Part I. The Effect of Fabrication Variables on the Anisotropy of Mechanical Properties," ORNL-2944, 1960, Oak Ridge National Laboratory, Oak Ridge, Tennessee.

48. M. L. Picklesimer, "Anodizing as a Metallographic Technique for Zirconium Base Alloys," ORNL-2296, May 24, 1957, Oak Ridge National Laboratory, Oak Ridge, Tennessee.

49. R. E. Reed-Hill and D. H. Baldwin, "A Technique for Orienting Grains in a Fine-Grained Polycrystalline Hexagonal Close-Packed Metal Using the Polarized-Light Microscope," Trans. Met. Soc. AIME, 1965, vol. 233, pp. 842-4.

50. E. E. Underwood and W. C. Coons, "The Role of Quantitative Stereology in Deformation Twinning," Deformation Twinning, pp. 405-29, Gordon and Breach Science Publishers, New York, 1964.

51. J. C. Bokros, "Critical Recrystallization of Zirconium," Trans. Met. Soc. AIME, 1960, vol. 218, pp. 351-3.

52. C. R. Simcoe and D. E. Thomas, "The Tensile Properties of Zirconium Alloys at Fabrication Temperatures and Strain Rates," WAPD-51, 1952, Westinghouse Atomic Power Division, Pittsburgh, Pennsylvania.

53. F. N. Rhines and P. J. Wray, "Investigation of the Intermediate Temperature Ductility Minimum in Metals," Trans. ASM, 1961, vol. 54, pp. 117-28.

54. R. E. Reed-Hill, E. R. Buchanan and F. W. Caldwell, Jr., "A Quantitative Measurement of the Fraction of Tensile Strain Due to Twinning in Polycrystalline Zirconium at 77°K," Trans. Met. Soc. AIME, 1965, vol. 233, pp. 1716-8.

55. A. H. Cottrell and R. J. Stokes, "Effects of Temperature on the Plastic Properties of Aluminum Crystals," Proc. Royal Soc. London, 1955, Series A, vol. 233, pp. 17-34.

56. C. A. Hampel, Rare Metals HandBook, Reinhold Publishing Corporation, New York, 1954.

57. C. Kittel, Introduction to Solid State Physics, 3rd ed., John Wiley and Sons, New York, 1966.

58. J. A. Cowan, A. T. Pawlowicz and G. K. White, "Thermal Expansion of Polycrystalline Titanium and Zirconium," Cryogenics, 1968, vol. 8, pp. 155-7.

59. E. S. Fisher and C. J. Renken, "Single-Crystal Elastic Moduli and the hcp-bcc Transformation in Ti, Zr, and Hf," Phys. Rev., 1964, No. 2A, vol. 135, pp. A482-94.

60. F. Povolo and E. A. Bisogni, "Internal Friction in Zirconium-Hydrogen Alloys at Low Temperatures," J. Nucl. Materials, 1969, vol. 29, pp. 82-102.

61. D. R. Miller and K. M. Browne, "Stress Induced Diffusion of Carbon and Oxygen in Titanium," International Conference on Titanium, London, May 1968.

62. J. N. Pratt, W. J. Bratina and B. Chalmers, "Internal Friction in Titanium and Titanium-Oxygen Alloys," Acta Met., 1954, vol. 2, pp. 203-8.

63. D. Lee, "The Strain Rate Dependent Plastic Flow Behavior of Zirconium and Its Alloys," Fall Meeting of the Metallurgical Society of AIME, Philadelphia, October, 1969.

64. B. Ramaswami and G. B. Craig, "Thermally Activated Deformation of Alpha Zirconium," Trans. Met. Soc. AIME, 1967, vol. 239, pp. 1226-31.

65. C. W. MacGregor and J. C. Fisher, "Tension Tests at Constant True Strain Rates," Trans. ASME, 1945, vol. 67, pp. A217-27.

66. J. W. Pugh, "The Tensile Properties of Molybdenum at Elevated Temperatures," Trans. ASM, 1955, vol. 47, pp. 984-1001.

67. J. W. Pugh, "Temperature Dependence of the Tensile Properties of Tantalum," Trans. ASM, 1956, vol. 48, pp. 677-88.

68. J. W. Pugh, "Temperature Dependence of the Tensile Properties of Vanadium," Trans. Met. Soc. AIME, 1957, vol. 209, pp. 1243-4.

69. S. A. Bradford and O. N. Carlson, "The Role of Oxygen in Strain Aging of Vanadium," Trans. Met. Soc. AIME, 1962, vol. 224, pp. 738-42.

70. D. Mills and G. B. Craig, "The Plastic Deformation of Zirconium-Oxygen Alloy Single Crystals in the Range 77° to 950°K," Trans. Met. Soc. AIME, 1968, vol. 242, pp. 1881-90.

71. D. A. Woodford, "Strain-Rate Sensitivity as a Measure of Ductility," Trans. ASM, 1969, vol. 62, pp. 291-3.

72. W. A. Backofen, I. R. Turner and D. H. Avery, "Superplasticity in an Al-Zn Alloy," Trans. ASM, 1964, vol. 57, pp. 980-90.

73. R. E. Reed-Hill, "Plastic Deformation in Titanium and Its Relation to Dynamic Recovery, Work Hardening and the Cottrell-Stokes Law," Second Technical Report to the Air Force Materials Laboratories, Wright-Patterson Air Force Base, October 10, 1969.

74. J. D. Baird and C. R. MacKenzie, "Effects of Nitrogen and Manganese on the Deformation Substructure of Iron Strained at 20°, 225°, and 450°C," J. Iron and Steel Inst., 1964, vol. 202, pp. 427-36.

75. B. J. Brindley and J. T. Barnby, "Dynamic Strain Ageing in Mild Steel," Acta Met., 1966, vol. 14, pp. 1765-80.

76. A. S. Keh, Y. Nakada, and W. C. Leslie, "Dynamic Strain Aging in Iron and Steel," Dislocation Dynamics, pp. 381-408, McGraw-Hill, Inc., New York, 1968.

77. J. W. Edington and R. E. Smallman, "The Relationship between Flow Stress and Dislocation Density in Deformed Vanadium," Acta Met., 1964, vol. 12, pp. 1313-28.

78. B. A. Wilcox and G. C. Smith, "The Portevin-Le Chatelier Effect in Hydrogen Charged Nickel," Acta Met., 1964, vol. 12, pp. 371-76.

BIOGRAPHICAL SKETCH

V. Ramachandran was born February 15, 1932, at Pudukkottai, Madras State, India. He graduted from Sri Brahadambal High School at Pudukkottai in 1947. In 1951, he received the degree of Bachelor of Science with major in Chemistry with First Class from the University of Madras. After serving as an Instructor at St. Joseph's College, Trichinopoly, for two years, he joined the Indian Institute of Science, Bangalore, in 1953, and received the Diploma of the Institute in Metallurgy in 1955. He was on the Faculty of the Department of Metallurgy, Indian Institute of Science from 1956 to 1966, as Senior Research Assistant, Lecturer and Assistant Professor. During this tenure, he came to the United States of America in 1961 on an Exchange Program for Teacher's Training sponsored by the United States Agency for International Development and received the degree of Master of Science with major in Metallurgical Engineering from the Michigan State University in 1962. He joined the University of Florida in 1966, and completed the doctoral studies, supported by a contract of the United States Atomic Energy Commission.

V. Ramachandran is married to Lakshmi. He is the father of two sons, Guruprasad and Krishnaprasad. He is a member of the American Institute of Mining, Metallurgical and Petroleum Engineers, American Society for Metals, the Indian Institute of Metals, Sigma Xi and Alpha Sigma Mu.

This dissertation was prepared under the direction of the chairman of the candidate's supervisory committee and has been approved by all members of that committee. It was submitted to the Dean of the College of Engineering and to the Graduate Council, and was approved as partial fulfillment of the requirements for the degree of Doctor of Philosophy.

March, 1970

Robert E. Uhrig
Dean, College of Engineering

Dean, Graduate School

Supervisory Committee:

R. E. Reed-Hill
Chairman

Arun Kumar Varma